
HOST UNIVERSITY: The University of Queensland

FACULTY: Engineering, Architecture and Information Technology

DEPARTMENT: School of Civil Engineering

Academic Year 2016-2017

# Effectiveness of Activation for Thin Intumescent Coatings

Nemer Abusamha

Promoter(s):

Dr. Cristian Maluk

Prof. Bart Merci

Master thesis submitted in the Erasmus+ Study Programme

**International Master of Science in Fire Safety Engineering**

# *DISCLAIMER*

This thesis is submitted in partial fulfilment of the requirements for the degree of *The International Master of Science in Fire Safety Engineering (IMFSE)*. This thesis has never been submitted for any degree or examination to any other University/programme. The author(s) declare(s) that this thesis is original work except where stated. This declaration constitutes an assertion that full and accurate references and citations have been included for all material, directly included and indirectly contributing to the thesis. The author(s) gives (give) permission to make this master thesis available for consultation and to copy parts of this master thesis for personal use. In the case of any other use, the limitations of the copyright have to be respected, in particular with regard to the obligation to state expressly the source when quoting results from this master thesis. The thesis supervisor must be informed when data or results are used.

Signature: 

Read and approved.
Date: April 30, 2017.

*This page is intentionally left blank.*

# *Abstract [English]*

Thin intumescent coating used for fire protection of steel structures swells during exposure to heat. Protection is derived from the swelling insulating layer that delay the heat transfer from the gas phase into load-bearing steel elements. However, there is limited understanding in the early stages of the intumescence process which promote an effective swelling activation of thin intumescent coatings.

This work investigates the occurrence and behaviour of swelling activation for thin intumescent coating under range of heating conditions in which incident radiant heat flux was carefully controlled and monitored. A heat transfer model allowed for estimations of accumulative thermal energy flux prior to activation.

Results show that swelling activation occur for an accumulative thermal energy flux of 12-13 $MJ/m^2$, when the steel temperature was in a range of 180-240$^oC$. Test results also showed that no swelling activation occurred when incident radiant heat flux was kept below 23 $KW/m^2$, indicating a threshold for swelling activation heat flux. Moreover, this study also assessed the swelling rate for tests in which activation was achieved.

# *Abstract [Arabic]*

الدهان الخارجي القابل للانتفاخ عند التعرض للحرارة لابنيه الحديد يستخدم لحماية اجزاء الحديد في البناء في حالة حدوث حريق. حيث يقوم الدهان بالانتفاخ و تكوين طبقه فحمية سميكة تقوم بتقليل انتقال الحرارة من الحريق الى حديد البناء لتقليل ازياد درجة حراره الحديد. لكن هناك عدم او قلة فهم صحيح لطريقة انتفاخ الدهان و بالاخص المراحل الاولى للانتفاخ التي تسمى المرحلة النشاطية.

تركزت محور هذه الرسالة على دراسة حدوث المرحلة النشاطية عند تعرض الدهان لاشعاعات حرارية متفاوتة النسبة, حيث تم التحكم بمقدار هذه الاشعاعات من خلال اله تحكم دقيقة. تم تصميم نموذج حسابي يسمح بتقدير تدفق الطاقة الحراريه التراكمية لما قبل المرحله النشاطيه.

اظهرت النتائج ان المرحلة النشاطية تحدث في نطاق معين من تدفق الطاقة الحراريه التراكمية [12-13] ميجاجول\متر مربع, وذلك عندما تكون درجة حرارة الحديد ما بين [180-240] درجة مئوية. ايضا اظهرت النتائج ان لا حدوث للمرحلة النشاطية عندما يكون الاشعاع الحراري دون 23 كيلوواط\متر مربع التي تبين حدود المرحلة الفاصلة للمرحلة النشاطية. جدير بالذكر ان هذه الرسالة بحثت ايضا في مرحلة الانتفاخ للاختبارات التي تم حصول انتفاخ فيها.

***Dear Dad,***

*شَكَوْتُ إِلَى وَكِيعٍ سُوءَ حِفْظِي - فَأَرْشَدَنِي إِلَى تَرْكِ المعَاصي*
*وَأَخْبَرَنِي بِأَنَّ العِلْمَ نُورٌ - ونورُ الله لا يهدى لعاصي*

***I would like to tell you that by writing this means that I am finishing my master's study, thank you. I dedicate it all for you.***

***Thank you for raising me up and always being there for me, thanks for sacrificing what you had to help me climbing the stairs of this life, thank you for giving me the chance to make me spread my wings and see the world, thank you for being the most kind and affectionate person ever in my life. You were the one who taught me since my childhood that knowledge and education are the keys for any locked door in this life, you were the one who taught me that patience is the key to overcome difficulties in this life.***

***I would like you to know that seeing you for the first time in my life laid down on the bed in the hospital with all these devices on you was the most difficult seen at all, it was the first moment in my life where I felt handcuffed and not able to do anything, I felt I wasn't able to do anything to save you except praying to Allah all the time. I wish that I have spent the past seven years of my life next to you rather being away from home, but I know you wanted me to do so and were proud of that.***

***Allah only knows that I was working on this thesis with tears in my eyes all the time, Allah only knows that I didn't give myself the chance to accept the fact you're gone for ever, I just wanted to finish what you wanted me to do and yes I did, I did with pain and sadness that's always inside me but decided to be put aside and get this done.***

***I wish to see you in the Heaven, and hug you for ever.***

***Love you Dad,***

***Your faithful son,***

***Nemer***

# *Acknowledgements*

***First of all, I would like to thank and praise Allah "God" for his guidance and inspiring me with strength and patience along this tough journey, he has given me strength after weakness, rising after falling and brightness after darkness during this challenging time of my life.***

***I would like to thank my family, mother, sister and brothers for their support during this challenging time, it wasn't easy to leave them at the time they needed me and at the time a huge gap existed in our lives after my dad.***

***I would like to thank Prof. Jose Torero and Prof. Bart Merci for giving me the chance to come to work at The University of Queensland and with the amazing UQ Fire group, thanks for making it possible and for this master program and the amazing journey you have provided for me.***

***I would like to give a sincere and special thanks to Dr. Cristian Maluk for his consistent and crucial feedbacks during this work, his supervision was a key to have this work done at any single point during the work, and it was pleasure and honour to work with such an intelligent person. ¡Muchas! mi amigo.***

***Also, I would like to thank PhD student Andrea Lucherini for his support and advises along the way, thanks Lucherini for being there all the time I needed.***

***I would like to thank the fire lab manager Jeronimo Carrascal Tirado for his assistance in making the H-TRIS work in the last moments and made it possible to carry this job and getting it done, also for his caring to make sure everything goes fine.***

***Also, I would like to thank all the technicians and workers who have participated in making things go in the right direction, those who I know and I don't know.***

***I would like to thank the people who joined me during the journey in this program, the IMFSE colleagues, thanks for sharing the good and the bad moments.***

***Lastly, I would like to give a sincere thanks to everyone in the UQ fire group Dr. Juan and the rest to draw a smile over my face during the challenging time, to provide a support and being very kind and friendly. Gracias.***

# *Contents*

# *List of Notations:*

| | |
|---|---|
| $Bi$ | Biot number |
| C | Specific heat |
| $C_{st}$ | Steel specific heat |
| $C_{ins}$ | Insulation Material specific heat |
| $F_o$ | Fourier number |
| $g$ | Gravitational acceleration |
| $h_c$ | Convective Heat flux |
| i | Subscript for time step |
| j | Subscript for element position |
| $k_{air}$ | Air thermal conductivity |
| $k_{st}$ | Steel thermal conductivity |
| l | Characteristic length of convective heat transfer |
| N | Total number of elements |
| $\overline{Nu_L}$ | Average Nusselt number at L length. |
| $Pr$ | Prandtl Number |
| $\dot{q}''_{inc}$ | Incident heat flux |
| $\dot{q}''_{loss}$ | Heat loss |
| $\dot{q}''_{net}$ | Total net heat flux |
| $Ra_L$ | Rayleigh number |
| $T_\infty$ | Ambient temperature |
| $T_j^{\,i}$ | Temperature at time i and element |
| $T_f$ | Film temperature |
| $\beta_{air}$ | Air volumetric thermal expansion coefficient |
| $\Delta t$ | Time Step |
| $\Delta x$ | Element size |
| $\varepsilon$ | Surface Emissivity |
| $\rho$ | Density |
| $v_{air}$ | Air viscosity |
| $\propto_{air}$ | Air thermal diffusivity |

# *List of Figures:*

## *List of Tables:*

# 1. Introduction

## 1.1 General Overview

The design of fire safe structure is driven by the need to mitigate the risks and hazards resulting from structural fires and allow for the elements of the fire safety to behave accordingly. Although not often when they occur, fire-induced structural failures have disastrous consequences; for examples; the Windsor fire in Madrid that was partially collapsed due to fire in 2005 (Anon n.d.). Current method for designing and constructing fire safe structures aims to primarily protect occupants, properties and ease the way for fire fighters intervention.

So-called active and passive fire protections systems are typically utilized in buildings. Active fire protection is based in the use of some sort of automatic or manual fire suppression systems that allows risk of a fully developed fire that might influence in structural performance (Buchanan 2001). Passive fire protection has to do with the design of structural fire performance and compartmentation by designing the load-bearing elements and separating elements of the structure (Buchanan 2001).

The use of insulating materials for protecting structure during and after fires has a widespread. Two types of insulation methods usually used when for steel structural systems; the use of inert insulation materials or the use of reactive insulation material (e.g. intumescent coating that swell upon heating).

Inert insulation systems traditionally have a high impact in the appearance of the structure; moreover, weight of the passive protection is sometime considered as an additional load to the requirements of the structure (Goode 2004). The use of reactive intumescent coatings has taken considerable attention across the construction industry. One of the most widespread reactive insulation materials are thin intumescent coatings that's widely used in the built environment.

Intumescent coating usually designed to swell when it's exposed to a certain level of heat and temperature which result in forming a char layer acts an insulation material which has the ability to minimize/stop the heat transfer to the substrate layer. Most of the non-reactive insulation materials are temperature dependent (Nørgaard 2014) and the thermal properties can be easily obtained by using of the standard tests. When it comes to reactive thermal insulation materials, situations can be different somehow. These materials is not only temperature dependent but can be also be a fire dependent which its temperature can vary significantly.

The work described herein studies the effectiveness of the thin intumescent coating under different ranges of heating conditions. More specifically, the work in this thesis, focuses on the initial stages of the process of intumesce; activation stage. A novel test method was design and construct, and heat transfer analysis of the thermal conditions during testing was carefully investigated.

## 1.2 Motivation and Research Need

The main driving force behind this research is the limited understanding of the effectiveness of swelling activation and swelling rate behaviour of thin intumescent coating.

The following diagram gives an explanation of the role of these intumescent coatings in fire safe structures.

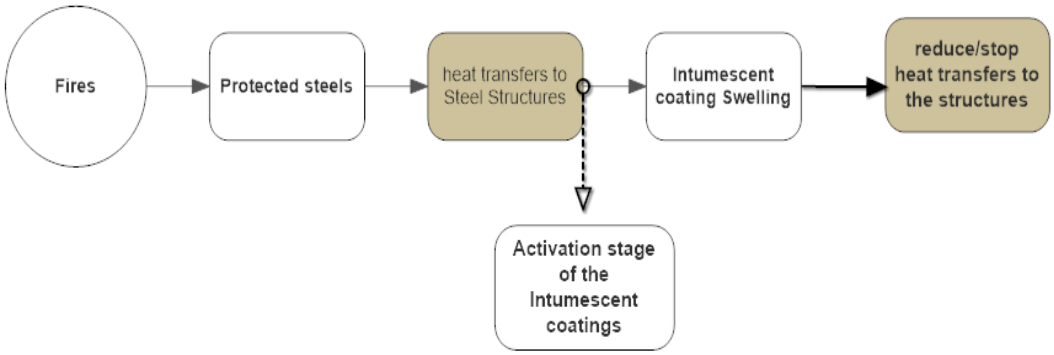


*Figure 1. 1: Event diagram for explaining the relevance of intumescent fire protection systems in steel structures.*

The above figure shows the importance of intumescent coatings in general which the benefit of the intumescent coating is given by the potential for delaying or limiting the temperature of load-bearing steel elements. Activation stage it's the major initial steps in the intumescence process as will be explained in later sections. Despite large amount of work from the fire science community, there has been little investigation assessing the activation and swelling behaviour of thin intumescent coatings for a range of heating conditions.

The main objectives of this work are to investigate:

- The occurrence and characteristic of the swelling activation under a range of heating conditions;
- Swelling rate behaviour under a range of heating conditions.

The accomplishment of these objectives will be obtained through the use of a H-TRIS (heat-Transfer Rate Inducing system) recently constructed for the Fire Laboratories at the University of Queensland, Australia. The novel heating system is described in the following sections.

## 1.3 Outline of the Thesis

This work focuses on studying the activation of thin intumescent coatings under ranges of heating scenarios. Section 2 presents a thorough literature review where passive fire protection systems for steel structural systems are presented. General overview of thin intumescent coating will be presented as well. Section 3 covers the experimental test method and a heat transfer model developed to describe the fire testing conditions. H-TRIS described, coated steel plates preparation will also be discussed. Section 4 presents the results from the thesis. Chapter 5 discusses the analysis that has been done over the results obtained from the tests. Section 6 discusses the conclusion and proposed future work.

# 2. Literature Review

Destruction due to fires can have significant consequences in life safety and property protection. The occurrence of an uncontrolled fire can its origins be driven by numerous situations and have the potential of affecting multiple aspects of a building or structure. In order to have a better understanding of how to understand and mitigate the effects of fire, the field of fire safety engineering and science has risen up during the past decades (Skowronski 2001). SFPE defines the fire protection engineering as "*the application of sceince and engineering principles to protect people and their environemnt from destructive fires"* (Richardson 2003). The main aim of structural fire safety engineering is to provide safe conditions for egress of ocupants, firefighting service intervention, and consider the potential need for property protection and business continuation. Two methods are typically employed to achieve this aim: active and passive fire protection.

Active fire protection commonly defined as the use of automatic or manual devices that *active* during fire; e.g. suppression system, smoke extraction system. The main challenges of active fire protection systems are (Buchanan 2001):

- Requires time to operate which can result In huge difference in terms of fire developemnt; and
- It's a system based on a sequence of operations lead to final direct of extinughsing the fire, and any fault in this chain can result in the system not working.

On the other hand, passive fire protection engolfes systems that are built within the structures, it doesn't require any sort of activation and are passive components of fire safety systems; e.g. insulation of structural system; natural ventillation designs. When it comes to steel structural systems, passive fire protection are built-in systems that insulate load-bearing steel structural components. The aim of utilising passive fire protection is to keep low temperature of the steel structural components. Active and passive fire protection systems can be combined in fire protection designs which can effectively reduce the risks and concequences of a fire (Ramachandran 1998). One of the most used fire passive systems in steel structures is the fire inuslation; explained in the context of the steel industry in the built environemtn in coming sections.

## 2.1 Fire performance of steel structures

Steel structures represent a large fraction of the consutruction industry; the high strengh and ductility of modern steel makes it the backbone of the built environment. The capabality for pre-fabrication of the steel that enhance the reduction of cost and time in consutrction has added more value for the use for the steel in construction. Steel is also an enviroment friendly, they can be recycled and don't release any pollutants during their design life (Industrial 2006).

However, exposure of steel to fire can subject it to thermally induced conditions that might alter its thermal properties. Steel at elevated temperatures can heavily alter the thermal properties of the steel, steel has a high conductivity which allows the steel temperature to rise up quickly which has a negative effect on its load carrying capacity. Loss of strength and stiffness of steel can lead to the partial or complete failure of structural systems. The rate of temperature increase depends on the severity of fire, the area of the exposed steel, and the amount of fire protection (Buchanan 2001).

The thermal properties of steel that are mainly influenced by the exposure to high temperatures are the thermal conductivity, specific heat and density as shown in Figure 2.1 below.

Moreover, the mechanical properties that affect the fire performance of steel are: strength, modulus of elasticity, coefficient of thermal expansion, and creep of component materials at high temperatures. One of the methods to assess the strength of the steel at high temperatures is the strength reduction factor versus temperatures. Strength reduction factor is the ratio of the strength at high temperatures to that at ambient room temperatures. Figure 2.2 shows the strength factor for hot rolled steel where it can be seen that the steel loses approximately half of the value of the strength compared to the value at ambient temperature.

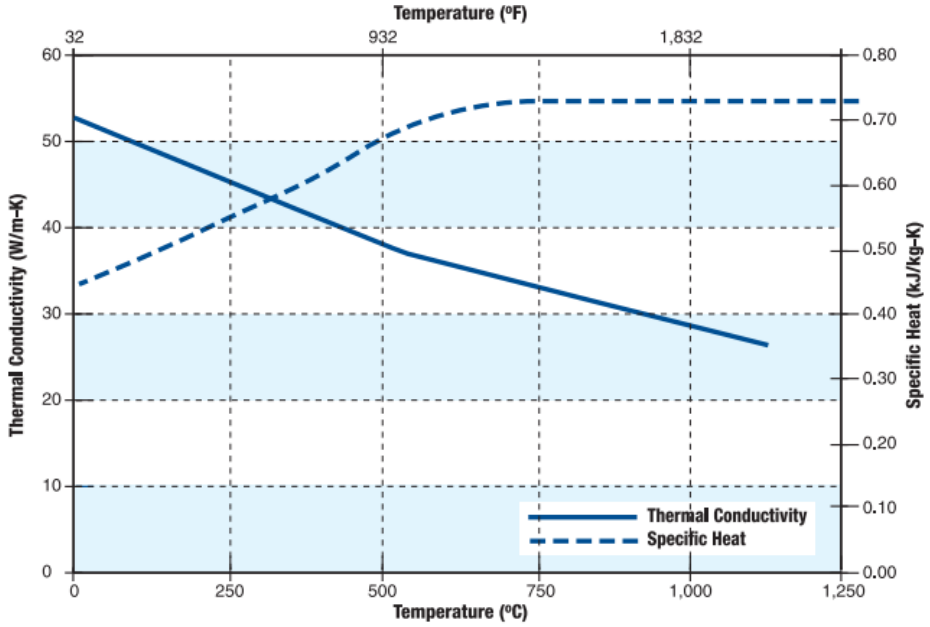


*Figure 2. 1: Thermal properties of steel at high temperatures (SFPE 2000).*

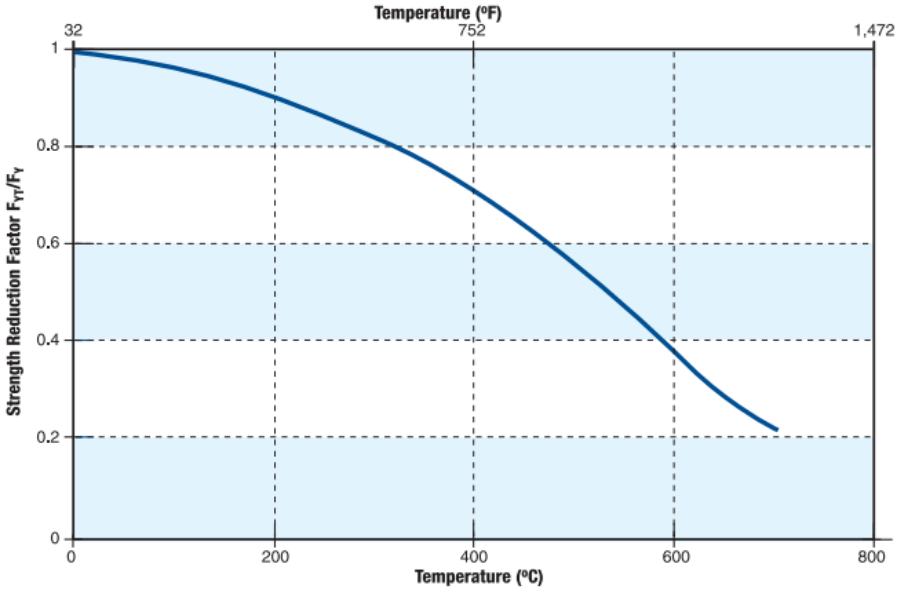


*Figure 2. 2: Strength reduction factor VS. Temperature (SFPE 2000).*

## 2.2 Fire Insulation materials for Steel Structural systems

One of the most common methods to protect steel structures is applying insulation materials that can sustain high temperatures and delay (or limit) the temperature increase of steel. There are a range of commercially available steel protection systems, in general fire insulation materials can be divided into two branches:

- Inert insulation materials; and
- Reactive insulation materials that swell upon heat exposure, creating an insulated media.

### 2.2.1 Inert insulation materials

In the past, asbestos was used to be sprayed over steel structures for providing appropriate fire protection. Nowadays, seriously health hazards have been noticed from using asbestos which resulted in banning it (Purkiss & Li 2013). Gypsum is used as good and cheap fire insulation material, the high quantity of water (21%) that's accompanied with gypsum base makes a high amount of energy needed to release this chemical composition as a steam. As the steam will not exceed 100$^{o}$C which gypsum can act well in the case of fire event, even after all the water is released from the gypsum, gypsum board is capable of acting as a fire resistant(Anon 2017). Figure 2.3 shows the process of heat transfer reduction mechanism by the gypsum.

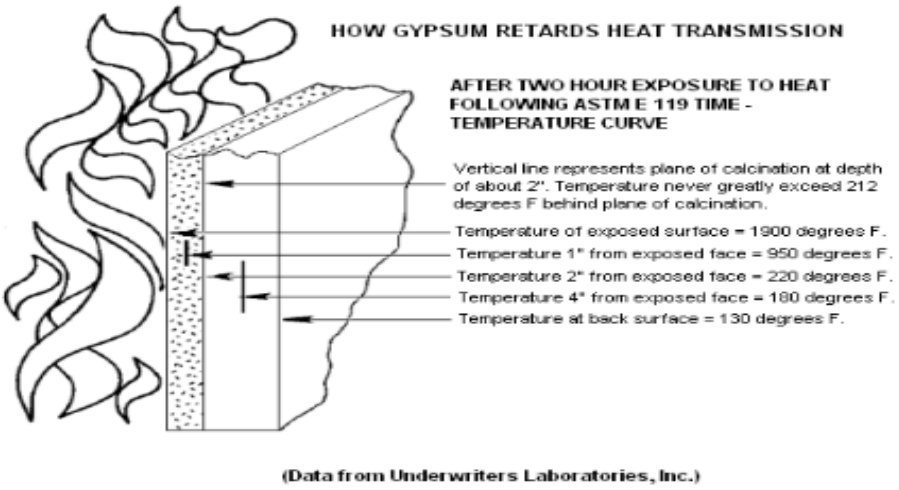


*Figure 2. 3: Heat Transfer reduction mechanism through the Gypsum (Anon 2017)*

Concrete encasement is also more traditionally used to protect steel. Concrete has a similar thermal advantage to that of gypsum, it evaporates water for the compensation of absorbing heat. Concrete transmit heat to the substrate layer in slow process as it has a low thermal conductivity. So increasing the thickness of concrete results in increasing the time required for the heat to reach the steel (Goode 2004). According to Buchanan (2001) this type of steel fire protection is well established and is applied widely. Moreover, durability is also an advantage aspect of concrete when it comes to corrosion.

One the other hand, there are significant disadvantages with concrete encasement; space issues, in other words, concrete requires significant space around the structural elements. It also takes a lot of time to install, weight of the concrete increases the weight of the structures. Cost of the concrete encasement is quite high. In addition, concrete spalling is one of the issues that has to be taken into consideration (Goode 2004). Figure 2.4 shows concrete encasement.

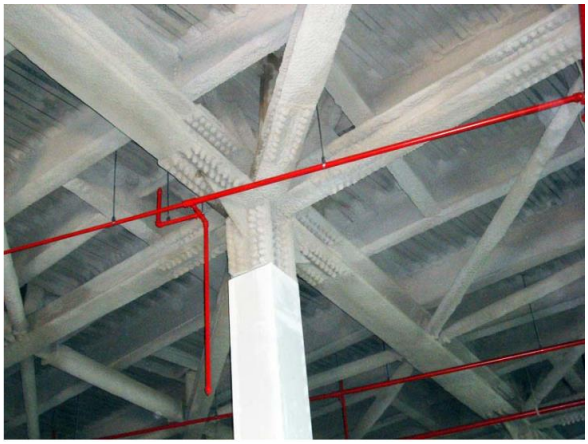

*Figure 2. 4: Concrete Encasement. (Anon 2017)*

One of the most traditionally site applied materials are the spray applied fire-resistive materials (SFRM). The main aim behind the use of these materials to delay/prevent the failure of steel structural' elements when it's exposed to elevated temperatures in the event of a fire. SFRM materials mainly composed of cement or gypsum and often contains other materials like mineral wool, quartz, perlite or vermiculite. Majority of the composition of the SFRM is made of gypsum or cement as explained earlier that it can hydrate the water inside which make both materials act as an insulation layer. SFRM available in both wet and dry spray (Archtoolbox n.d.)

The challenging side with the SFRM that it requires intensive labour works to have good quality, also it can't be applied at surfaces that are exposed to moisture or high humidity levels which can break down the spray. Also, the moisture can cause mould growth due to the high porous surface of the materials (Wang 1995). Figure 2.5 shows Spray protection systems on-site.

*Figure 2. 5: SFRM on-site. (NIST 2005)*

Buchanan (2001) indicated that increasing the heat capacity of the steel structures' elements can be done by filling inside a hollow structural elements that act as a heat sink. They can be filled either with water or concrete. The process of fire resistant through this process is as follow; the heat passed through the exposed steel, then accumulates within the fillings, when the yield strength of the steel go down, the load is transmitted to the fillings. Disadvantage of this method is increasing the weight of the structure.

Generally stating, the fire insulation materials have some major disadvantages such as weight, appearance, difficultly to apply, exposed to shatter and spalling when exposed to fire.

### 2.2.2 Reactive insulation materials

One of the most efficient traditionally methods to protect steel structures are reactive insulation materials for a variety of reasons:

- Light weight which doesn't add any load to the structure.
- Low cost compared to other inert insulation materials.
- Easy to apply on site and off site and doesn't require many labour work to have the insulation over the steel structural components.

There are two main types of reactive insulation materials used in construction based on their usage: ablative and intumescent coatings.

Ablative coatings are used for protecting surfaces with short characteristics lengths (e.g. cables), and intumescent coatings used for sealing openings. For load-bearing steel structures both can be used for variant usages successfully. Intumescent coatings are explained in more detail below.

Ablative materials are endothermic materials where heat activate a series of chemical reactions within the materials that requires amount of thermal energy that's being absorbed in order to reduce the increase of temperature in the beneath layers. Steam is also released by the reactions which help to minimize the chance of having ignition at the surface. Thickness of ablative coatings ranges from 1-7mm based on the preferred protection time, 1-2mm usually protect from fires for almost 20 minutes. Resin Is usually applied at the surface In order to protect from water and mechanical damages, disadvantages of the these type of paint are in terms of cost and complexity to apply which has opened the doors for intumescent coating materials to appear on the surface to become preferred type of fire insulation materials in steel structures (Mroz et al. 2016).

## 2.3. Intumescent coatings

### 2.3.1 Development of Intumescent coating

Prior to the first scientific article on a civil engineering journal in the 1970s Vandersall, the concept of intumescence had only been used in other contexts. For example, the first to report the intumescent coating was Tramm et. al in 1938, and then Wang and Chow. Both discussed the components of the intumescent coating based on their function during the chemical reaction of the intumescence process, where they defined the "*carbonific*" and "*supimifcs*", both will be explained in detail in the following sections

Vandersall (1970) drawn the basics of the intumescence process, where it explained that intumescence process highly depends on a set of chemical compounds. Mariappan (2015) mentioned that many patents have been granted in the development of the intumescnet coating but still a big gap in understanding the performance of the intmescent coating exisits. Many of these patents granted in intumescent coatings have some limitations such as, weather sensitivity, poor thermal properties, high cost. However, an intensive research has been done over the past decades in order to study the intumescent coating and defining possible foundations that help for better understanding.

### 2.3.2 Overview and components of Intumescent coatings

Intumescent coatings have gained significant attention due to sufficient fire protection and low health hazards compared to other paintings. It has been used in Europe for more than 40 years, it provides a protection in the event of fire. The reasons that helped in high adaption In extensive using of the intumescent coating are; pleasant appearance, speed of applying during the construction, cost savings, corrosion protection and quality control, it can be also be applied on-site and off-site which can provide better finishing.

In general, the application of intumescent coatings has been growing since the beginning of this millennium compared to other protective materials, and that's due to the development of the intumescent coating which reduces the cost and increases the performance of the protection. Figure 2.6 shows the application usage of the intumescent coatings compared to the other fire insulation materials between the years 1992-2004 (steelconstruction.info 2016).

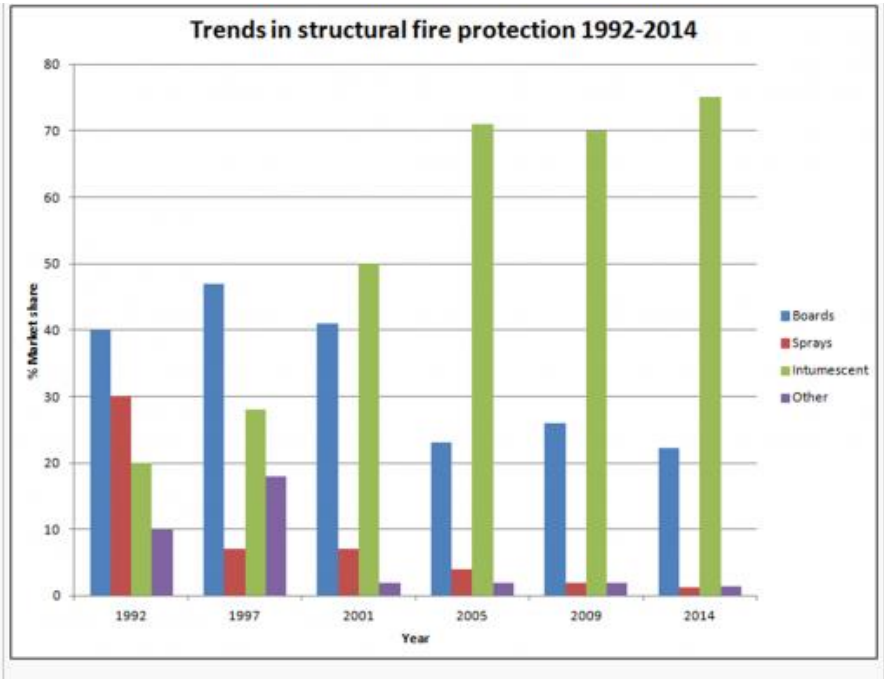


*Figure 2. 6: Percentage of the use of passive fire protection materials between the years 1992-2014 (steelconstruction.info 2016).*

Intumescent coating tends to expand when it's exposed to heat, hence minimize the transfer of heat to the substrate (i.e. steel structure). Intumescent coatings are usually designed to maintain steel integrity for one up to three hours when the temperature of the surroundings exceeds 1100C, the reason behind three hours can help in preventing the collapse of the structure or delaying the collapse until safe evacuation of occupants or/and giving time allowance for the fire brigade. Generally speaking, when the surface temperature of the coating reaches a critical temperature which activate the chemical reaction within the coating, the surface starts to melt to become very viscous, the final result of the series of the chemical reactions of the coating is a formation of a char which acts as a insulation layer to the substrate layer (Jimenez et al. 2006). Reactive coatings typically applied at dry film thickness of few millimetres, during fire will expand from 50-200 times their initial thickness (Elliott et al. 2014).

Two types of Intumescent coating commonly applied based on their usage and the type of fire the coating is expected to face; thin and thick intumescent coatings (steelconstruction.info 2016).

Goode (2004) mentioned two types for thin intumescent coatings; single part solvent based and single part water based. The former one typically implemented for exterior applications and interior applications and tested against weather and temperature gradients. The later one have less smell compared to the former one but less endurance for high temperatures. Thickness of thin coatings in the range of 1-3 millimetres.

Thick intumescent coatings are usually epoxy based, thickness is much larger than the dry thin intumescent coatings. It's mostly used in harsh environment, where a hydrocarbon fires may occur, and difficult access to maintenance. Cost of these materials are much higher compared to other intumescent coatings, the behaviour of the thick intumescent coatings is similar to the thin ones, but they are not classified same as thin due to the content of the epoxy. The thickness of the coatings is generally thicker and in the range of 5-25mm rang (Goode 2004). The expansion of these materials are typically 5 times compared to the initial (steelconstruction.info 2016).

Intumescent coating commonly has a combination of essential components that's works together to form the final inulsation layer (char), performance of the intumecent coating depends on the good choice of these combination. The following are usually exisiting in the intumescent coating (Mariappan 2015.);

- Catalyst/acid source; an organic acid/compound that melt to mineral acid on specific range of temperatures (i.e. 100-250$^{o}$C).
- Carbonific; carbon which contains carbon donor/charring agent with a large amount of phosphorous estrifiable sites which should break down at higher temperature than the acid source to have homogenous intumesce.
- Spumific/blowing agent; an organic compound that when decompose release a large amount of gases that cause carbonifc to bubble and foam, blowing should happen after the melt of the catalyst and before the gelation occurs.
- Binders; this forms a skin over the bubble face and assures that a homogenous foam structure throught the face.

It should be noted that these four different compositon may overlab during the intuemscent process and they are not narrowed only to what have been explanied above (Mariappan 2015)

### 2.3.3 Mechanisms of intumescence

Intumescent coating full expansion process is quite complex and still requires a lot of understanding. Basically, the general overview of the Intumescence process is to undergo an endothermic reaction at high temperatures that causing the coating to swell, foam and have a formation of thick, viscous char layer that has a low thermal conductivity. Generally, intumescent coatings undergo five different steps according to Anderson et al. (1985):

1. The catalyst melts/decompose to form an acid at temperatures in the range of 100 and 250$^{o}$C.
2. At around 300-350 degrees the acid react with the carbonicif to form esters by the dehaydration.
3. Ester decompose to from large volume of carbon and release the acid.

4. The blowing agent realese a large number of gases (e.g. $CO_2$, $NH_3$, water vapour, etc.) which result in forming the bubbles.

5. The expanding of the bubbles cause the carbon to expand and form a thick, visocus layer which act an insulation.

The following figure shows the intumescene process for the intumescent caoting during an exposure to an external heat flux due to the event of a fire, where as can be seen, the top layer starts to react when the critical temperature reached, then the swelling process starts to take a place due to the bubbling process, char starts to from over the intumescent coating face at the same time the reaction within the coating is taking place until no more reaction occur and a whole thick layer of char is formed. It should be highlited that would happen in the ideal case of the intumescne process.

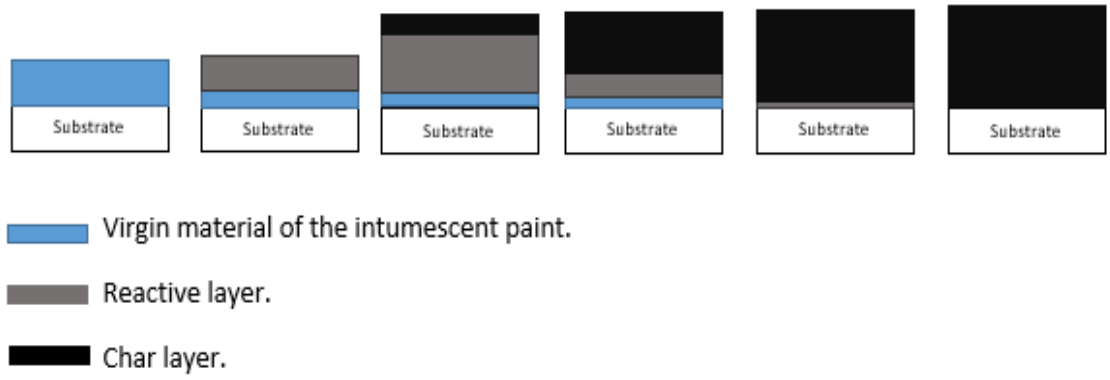


*Figure 2. 7: Intumescence process.*

The main feature of the whole intumescnece process is the formation of a thick, high carbon concetration, high viscous char layer that has low thermal conductivity. Another important aspect is the mechanical strenght of the intumesced char (Mariappan 2015).

The bubble size of the inumesced char highly effect the effecincy of the insulation, an early activiation of the blowing agent can result in having bubbles that will be bunred before expanison as the viscosity of the molten char is too low. On the other hand, the other bubbles that didn't burned would expand but providing insuffcient capability of fire protection (Cirpici 2015). Therefore, the acitivation temperature and the sequence of the activiation of each component is extremely important in order to have an efficient insultion intumecent coating.

Its also essential that the different component of the caoting should be carefully selected to have a successful activiation, a random selection of these componets wouldn't guranatee a successful acitiviation. For example, the blowing agent have to break down at higher temperature than which the charring of the compounds starts, at the same time before the solidification of the liquid charing melts (Jimenez et al. 2006).

### 2.3.4 Relevant studies on activation and swelling

The current movement of the world in the field of fire safety engineering is towards a performance based design fire engineering, and that's due to the deep gained knowledge of fire engineering in the past decades. Performance based approaches provide flexible, safer and more economical designs in steel structures. But performance base design takes into account different conditions than the standard tests do, such as type of fire, consequence of fire exposures, loading conditions and the

resultant interaction between the steel structural elements. That's why there is a passion to understand the performance of the intumescent coating under realistic fire conditions (Wang 2002)

However, few research and almost no work has been done on the study of the activation of the thin intumescent coating, but many work has been done on the intumescent coating performance in general. According to Jimenez et al. (2006) intumescent coating is not only a temperature dependent but also a fire type dependent which makes the study of intumescent coating under different ranges of fires challenging as the thermal properties of the intumescent coating is highly varied by the heat flux exposed. According to Wang (2005) experiment on intumescent coating by a series of cone calorimeter tests on protected steel plates, he found that the effective thermal conductivity of the intumescent coating (which is the apparent thermal conductivity divided by the expansion ratio to the original thickness) can differ more than 4 times with the same heat flux as shown in Figure 2.8. As can be seen in the below figure, the effective thermal conductivity versus. the steel temperature is plotted, where it shows that the effective thermal conductivity changes drastically with the steel temperature as the thermal conductivity increase and decrease with the increase of the steel temperature which makes It difficult to account for the activation.

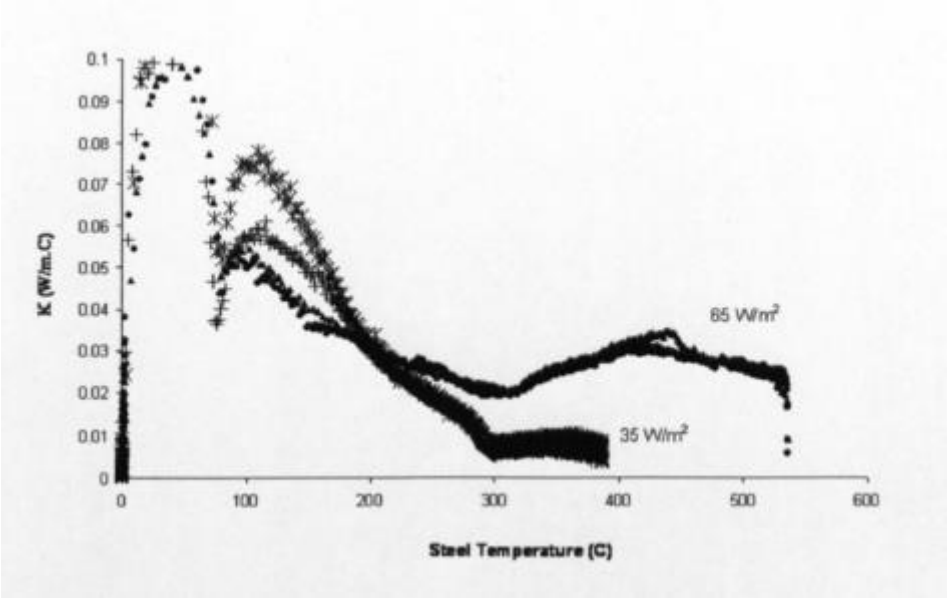


*Figure 2. 8: Effect of heat flux on the effective thermal conductivity of Intumescent coating. (Wang 2005).*

The above figure gives a clear indication that within the same heat flux the effective thermal conductivity is difficult to obtain which would make it more complicated under ranges of heating conditions.

As explained earlier, bubble generation and growth due to the chemical reactions within the intumescent coating is responsible to provide the charring layer to expand and provide a proper insulation, bubbling as terminology in intumescent coating is a resulting product of the interaction of the released gas from the blowing agent and the binder. Viscosity of the binder is a temperature dependent and has a lot of influence on the final expansion. The viscous supply resistance and control bubble growth (Horrocks 1996) which is eventually influence a homogenous activation of the intumescent coating. Moreover, so what called the ''chemical reaction kinetic'' that has to do with the reaction rate is highly influenced with the temperature which affects the bubble generation that depends on the chemical reaction during the intumescence process. Also, it's worth mentioning that the increasing temperature rate can also influence the intumescence process.

Wang l (2015) have focused on studying experimentally the performance of thin intumescent coating under different non-standard exposed furnace curves that was applied on steel plates and he has found out that the reaction steps that the intumescent coating would take depends highly on the maximum temperature reached and that the foaming degree of the char is highly effected by the heating conditions. In addition, he found out that increasing the coating thickness doesn't always provide better insulation compared to those would be exposed to standard tests.

Elliot et al. (2014) have studied the performance of the intumescent coatings under non-standard heating regimes using a novel fire test method, equivalent to the one used in this work. The investigation has been done on studying the effective thermal conductivity based on simulated test exposure from cellulosic, hydrocarbon and smouldering furnace and found out that heating rate and dry film thickness of the coating doesn't affect drastically the development of the effective thermal conductivity for the intumescent coating.

Lucherini (2016) has studied behaviour of steel structures protected by different intumescent coating exposed to various of heating conditions and has found out that thermal shielding of the intumescent coating is influenced by heat flux, coating thickness sample size.

Mcnamee and Storesund (2016) have done an experimental study over the performance of the intumescent coating that was applied on steel section and exposed to different fire scenarios using cone calorimeter, standardised furnace tests, ceiling jet and plume fire. The study showed that the adhesion was lost to two systems during the furnace tests, ceiling jet and plume fire, recommendation for further research over the adhesion was suggested.

Mesquita et. al (2007) has done an experimental study over the Intumescent coatings using different heating scenarios using cone calorimeter and different coating thicknesses, the study showed that the intumescence development highly depends on the initial dry film thicknesses and on the incident heat flux.

Previous researchers on intumescent coating have always focused on development that would make the intumescent coating overpass the standard resistance tests. Vandersall (1971) first to review the chemistry of intumescence and gave a general description of the chemical components. Camino et al (1986, 1988, and 1989) focused more on the mechanism of the intumescence process who highly contributed to the chemical aspect of the intumescence process. Le bras (1998, 2000) and Bourbigot (200, 2004) have focused on how different chemical components can influence the behaviour of the intumescent coating.

However, there is intensive research done on the modelling of the intumescent coating and the intumescence process using different approaches. However, this is beyond the scope of this work. The main focus of this work will be on studying the activation stage based on thickness and different heating conditions. Bubbling sizes and effective thermal conductivity will not be covered within the scope of this work but can be recommended in the future work recommendation section as will be shown later.

# 3. Methodology

Within the scope of this chapter, details of the experimental studies of this work are described. This chapter covers the following topics:

- Heat transfer analysis
    - Convective heat transfer
    - Biot number
- Experimental test setup
- Test procedure

## 3.1 Heat transfer analysis

A heat transfer analysis was performed in order to study the thermal boundary conditions at the exposed surface of the protected steel plates tested within the scope of this study. A 1-D numerical model was done using an explicit finite difference formulation. The outcomes of the 1-D model are the temperature variation of the steel and coating. The following assumptions were considered in the heat transfer model:

- Thin intumescent coating and steel are thermally thin; Biot number < 0.1 (this is verified in the following sections);
- The unexposed side of steel is considered to be adiabatic; no heat exchange;
- Intumescent coating was considered to remain with the same mass during exposure;
- Heat capacity, density, and thermal conductivity are not temperature dependent ; and
- Temperature dependent convective heat coefficient is calculated.

The plate was divided into N elements. The thickness of the boundary sides (exposed and unexposed) have the thickness of ΔX/2 with nodes located at the elements' edges. The interior elements have the thickness of ΔX that's located at the centre of the elements.

Figure 3.1 shows the discretization of the system into N elements. Note that

$$\dot{q}''_{net} = \dot{q}''_{loss} + \dot{q}''_{inc} \quad (1)$$

j is the node number and i is the time step.

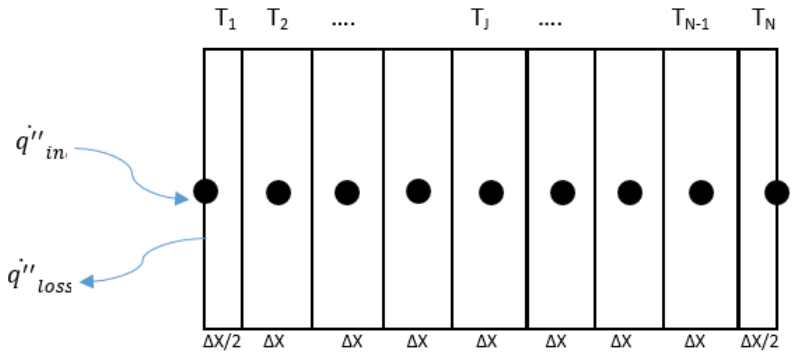


*Figure 3. 1: Finite difference method model.*

Energy balance equation was established for each node. $\dot{q''}_{inc}$ is the exposed heat flux over the thin intumescent coating at the first node per unit area. The set of equations was calculated as follows;

For Node 1 (exposed side) the energy balance is as follows;

$$\dot{q''}_{inc} - \dot{q''}_{loss} - k_{st}\left(\frac{{T_1}^i - {T_2}^i}{\Delta x}\right) = \rho_{st} C_{st} \frac{\Delta X}{2} \frac{{T_1}^{i+1} - {T_1}^i}{\Delta t} \quad (2)$$

$$\dot{q''}_{loss} = [h_c.({T^i}_1 - T_\infty) + \varepsilon\sigma({T^4}_i - {T^4}_\infty)] \quad (3)$$

Where $\varepsilon$ is the emissivity of the exposed side, and $\sigma$ is the Stephan-Boltzmann constant which is equal to 5.6704*10$^{-8}$[$\frac{J}{s.m^2.K^4}$].

For the interior elements, the energy balance equation is as follows;

$$k_{st}\left(\frac{{T_{j-1}}^i - {T_j}^i}{\Delta x}\right) - k_{st}\left(\frac{{T_j}^i - {T_{j+1}}^i}{\Delta x}\right) = \rho_{st} C_{st}.\Delta x.\frac{{T_j}^{i+1} - {T_j}^i}{\Delta t} \quad (4)$$

And for the unexposed face the energy balance equation is as follows;

$$k_{st}\left(\frac{{T_{N-1}}^i - {T_N}^i}{\Delta x}\right) = \rho_{st} C_{st}.\frac{\Delta X}{2}.\frac{{T_N}^{i+1} - {T_N}^i}{\Delta t} \quad (5)$$

Rearranging the above equations to find the temperatures at each node. At the exposed side;

$${T^{i+1}}_1 = {T^i}_1 + \frac{2.\Delta t}{\rho_{st} C_{st}.\Delta x}[\dot{q''}_{inc} - \dot{q''}_{loss} - k_{st}\left(\frac{{T_1}^i - {T_2}^i}{\Delta x}\right)] \quad (6)$$

At the interior elements;

$${T_j}^{i+1} = {T_j}^i + \frac{2.\Delta t}{\rho_{st} C_{st}.\Delta x}.[\, k_{st}\left(\frac{{T_{j-1}}^i - {T_j}^i}{\Delta x}\right) - k_{st}\left(\frac{{T_j}^i - {T_{j+1}}^i}{\Delta x}\right) \quad (7)$$

And at the unexposed surface;

$${T_N}^{i+1} = {T_N}^i + \frac{2.\Delta t}{\rho_{st} C_{st}.\Delta x}.[k_{st}\left(\frac{{T_{N-1}}^i - {T_N}^i}{\Delta x}\right)] \quad (8)$$

One of the undesirable feature of this explicit method is that it's not unconditionally stable, the solution may end up with induced oscillations which may cause the solution to diverge from reaching steady state solutions. This can be prevented by introducing a stability criterion which defines that $\Delta t$ must be maintained below a certain limit. In general, for one dimensional equation the dimensionless Fourier number has to be below a certain value or (1-2$F_o$) ≥ 0, Fourier number is calculated by the following expression;

$$F_o = \frac{k\Delta t}{\rho c \Delta x^2} \leq 0.5 \quad (9)$$

Which can result in the following expression;

$$\Delta t \leq \frac{\rho c \Delta x^2}{2.k} \quad (10)$$

The above criterion was calculated for the different properties of both thin intumescent coating and the steel plate; the time step has been chosen to be the lower between the both calculated values;

$\Delta t < \min(\Delta t_1, \Delta t_2)$, The inputs for all thermal properties for the steel has been obtained from the EN 1993.1.2 and EN 1991.1.1.

### 3.1.1 Biot Number and Convective heat transfer

In this work, the surface of the thin intumescent coating is exposed to free convection as the air motion is due to the buoyancy within the air, which is resultant of the density gradient within the air. As in the case here temperature is the driving force for the density gradient for the air over the surface of the coating.

At exposed surface of the thin intumescent coating, the convective heat transfer coefficient over a vertical plate is calculated as the following according to Bergman et al (2011) is calculated as follows;

$$h = \frac{\overline{Nu_L}.k_{air}}{L} \tag{11}$$

Where;

$$\overline{Nu_L} = \begin{cases} 0.68 + \dfrac{0.67.Ra_L^{\frac{1}{4}}}{\left[1+\left(\frac{0.492}{Pr}\right)^{\frac{9}{16}}\right]^{\frac{4}{9}}} & Ra_L \leq 10^9 \\ \left[0.825 + \dfrac{0.387.Ra_L^{\frac{1}{4}}}{\left[1+\left(\frac{0.492}{Pr}\right)^{\frac{9}{16}}\right]^{\frac{8}{27}}}\right]^2 & Ra_L > 10^9 \end{cases} \tag{12}$$

Where;

$$Ra_L = \frac{g\beta_{air}(T_i - T_\infty)L^3}{v_{air}.\propto_{air}} \tag{13}$$

Where L is the vertical height of the plate.

g= 9.81 m/s$^2$ (14)

$$\beta_{air} = \frac{1}{T_f} \tag{15}$$

$$T_f = \frac{({T_1}^i + T_\infty)}{2} \tag{16}$$

The convective heat transfer coefficient was calculated based on the maximum and minimum first element's temperature, so that an average value can be taken. It was found out that the range of the convective heat transfer coefficient wouldn't vary much based on the temperature, the range was [7-18] a rough assumption was taken to be 10 w/m$^2$.k. The air properties has been obtained from Bergman (2011)

### 3.1.2 Biot number

Biot number is a dimensionless number that represent that ratio of thermal resistances towards conduction and convection. If Bi << 1 it means that the *resistance to conduction within the solid is much less than the resistance to convection across the fluid boundary layer* (Bergman et al. 2011). And vice versa is correct.

Figure 3.2 shows the temperature variation within the body based on the value of the Biot number, this variation is strongly influenced by the Biot number value. It can be seen that for Biot number much less than 1 it can be assumed that temperature variation within the body is small and a uniform temperature distribution exist. For numbers close to 1 and much larger, the temperature variation within the body is significant where it can be seen that temperature within the solid is much larger than the one between the surface and the fluid (Bergman et al. 2011).

The Biot number can be calculated according to the following formula;

$$Bi = \frac{hL_c}{k_{body}} \tag{17}$$

Where $L_c$the characteristic length has been considered to be the DFTs or steel plate.

To sum up, thermally thin materials are called for materials which have a Biot number less than 0.1, which means physically that the temperature variation within the body is small and the temperature at the both sides can of the materials can assumed to be the same.

Where the characteristic length has been considered to be DFTs or steel plate. The calculation for Biot number has been for both the steel plate and the thin intumescent coating and it was noticed that both of the materials are thermally thin. The calculated Biot number for both Intumescent coating and the steel plates are 0.028 and 0.025 respectively. Both are less than 0.1 which indicates both are thermally thin.

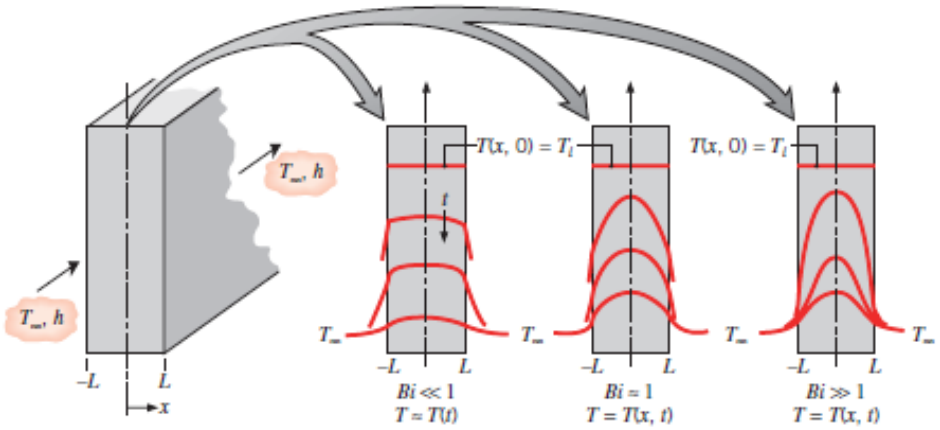


*Figure 3. 2: Temperature variation within a body based on the value of Biot number (Bergman et al. 2011).*

## 3.2 Experimental test setup

### 3.2.1 Test samples and fabrication

Unprotected carbon steel plates were manufactured for this work, the following table shows the number and the dimensions used, and the thin intumescent coating was sprayed manually by a professional painters using airless spray gun. The type of the thin intumescent coating that was used didn't really matter according to the main objectives of this work.

The plates were classified and arranged in different sets according to the desired DFTs (Dry-Film thickness). As mentioned before, thin DFTs of intumescent coating can be up to 3 mm. For this work, 1, 2 and 3 mms of intumescent coating were chosen to study the effect of the DFTs on the activation behaviour of the thin intumescent coating, but no necessarily the desired thicknesses have been used for the tests.

The professional painters used a comb wet film thickness gauge to keep tracking of the thicknesses during the spraying processes. It should be highlighted again this work is part of a bigger research work at the University of Queensland so not all the listed below protected steel plates have been tested, but the author of this work has participated in preparing and measuring the different thickness, thermal properties of the thin intumescent coating.

*Table 3. 1: Steel Plates dimensions.*

| | |
|---|---|
| Number of Plates | 115 plates |
| Thickness | 10 mm |
| Height | 200 mm |
| Width | 200mm |

*Figure 3. 3: Spraying process.*


*Figure 3. 4: Wet film thickness gauge comb.*

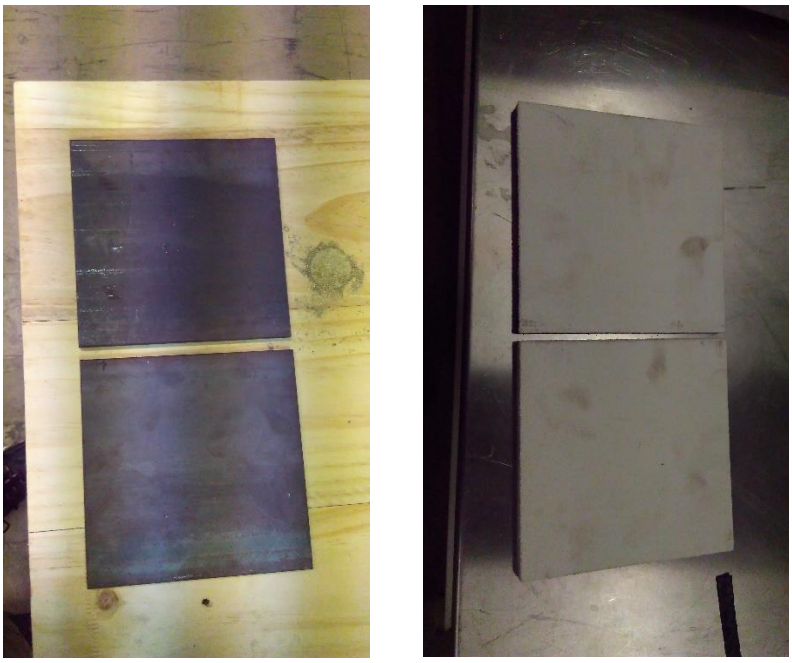

*Figure 3. 5: Protected and unprotected steel plates*

The plates were left for one week in the same place where the spraying process has taken place in order to dry; one week has been chosen to have confidentiality that the paint would take the necessary time to dry up. After that, the DFTs measurement were conducted using an Elcometer. Figure 3.6 shows a photo of the Elcometer used in this work. The results of the Elcometer have been listed in Appendix A, different 5 points throughout the plates were considered for measurements, and then average DFTs was considered as the DFT for the plate.


*Figure 3. 6: Elcometer.*

The thermal properties of thin intumescent coating were measured using the Hot Disk. Hot disk works as shown in (Anon 2014). The hot disk sensor is placed between the two identical pieces of the sample material, and then it's heated up by constant electrical current for a short period of time. The heat then dissipates to the surrounding material resulting in increasing the temperature of the sensor and the surrounding material. The change in the electrical resistance is observed continually in order to record the transient temperature.

The hot disk sensor was placed between two identical pieces of thin intumescent coating. The figures below show the thin intumescent coating materials and the sensor during the measurement. The Hot-disk gives the value of the thermal conductivity. The density was measured manually by measuring the weight of 1 $cm^3$ using weight scale. The specific heat was also measured using the hot-disk. The results from the hot-disk measurements based on average values taken are presented in the Table 3.2.

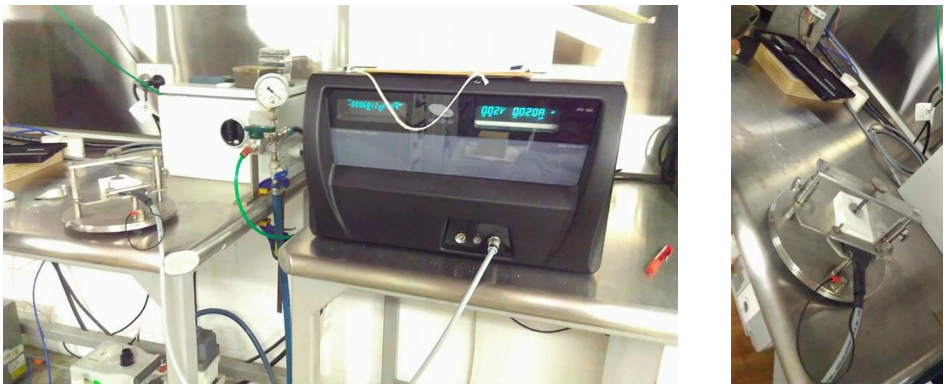

*Figure 3. 7: Hot-disk instrument at the university of Queensland-Australia.*

*Table 3. 2: Thermal properties measured for thin Intumescent coating.*

| **Thermal conductivity (W/m.k)** | **Specific heat (KJ/kg.k)** | **Diffusivity ($mm^2/s$)** | **Density ($Kg/m^3$)** |
|---|---|---|---|
| **0.52** | 1196 | 0.312 | 1471 |

### 3.2.2 Radiant panel

A *Heat-Transfer Inducing System* (H-TRIS) was used within the scope of this study. H-TRIS, unlikely standard test methods is controlling the thermal boundary conditions imposed on the test specimen by using prescribed time history of incident heat flux instead of prescribed time history of temperatures (Maluk et al. 2016).

The linear motion system in the H-TRIS allows to move the radiant panel furthest and closest distances relative to the specimen location, these distances give the maximum and minimum incident heat fluxes imposed on the specimen respectively. The incident radiant heat flux on the specimen is calibrated using water cooled Schimdt-Boetler heat flux gauge (Figure 3.10). The calibration procedure will be described in later section where more explanation shows the relative position of the radiant panel and the incident heat flux at the surface of the specimen.

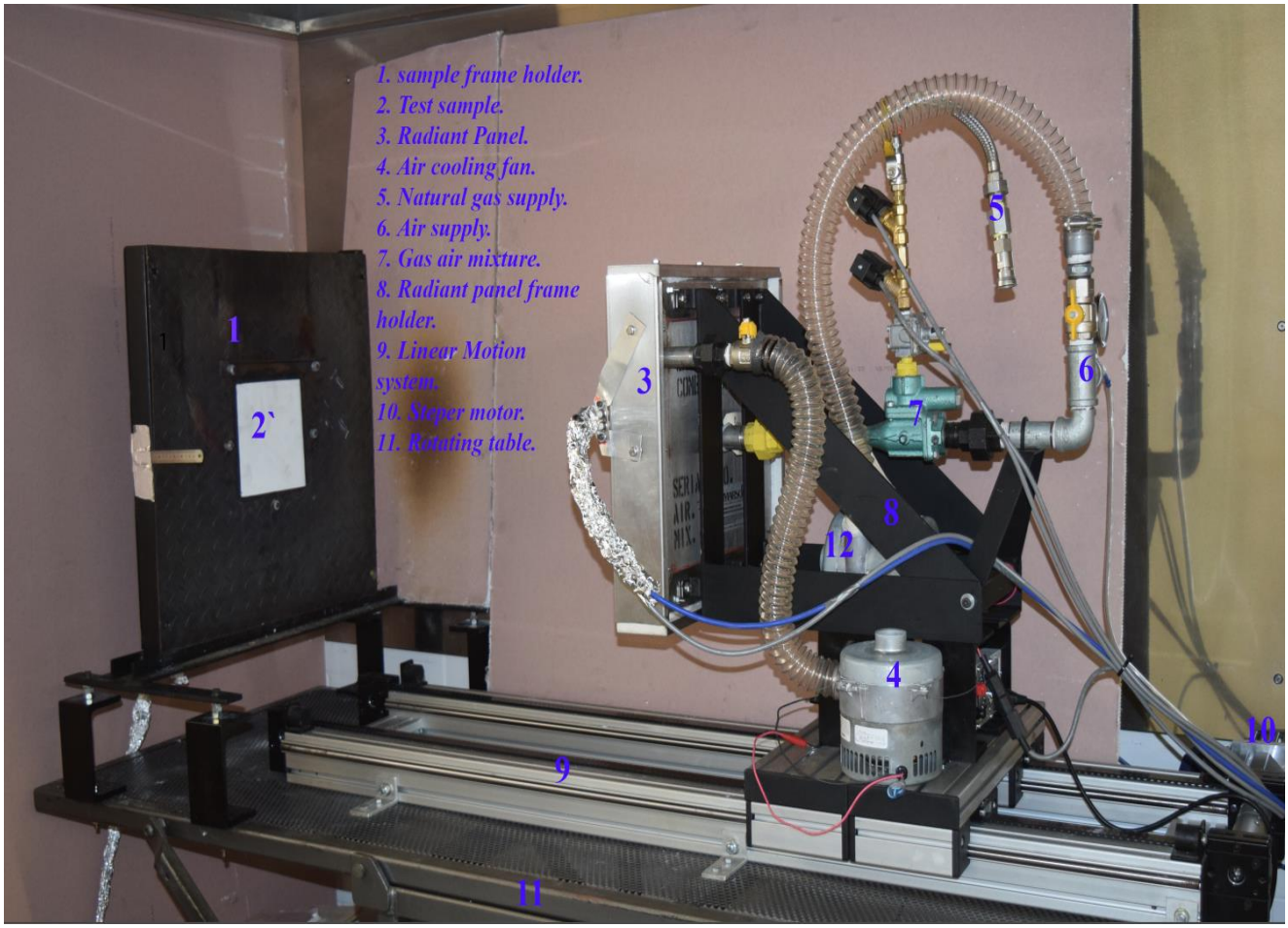


*Figure 3. 8: Photograph showing the test setup (H-TRIS).*

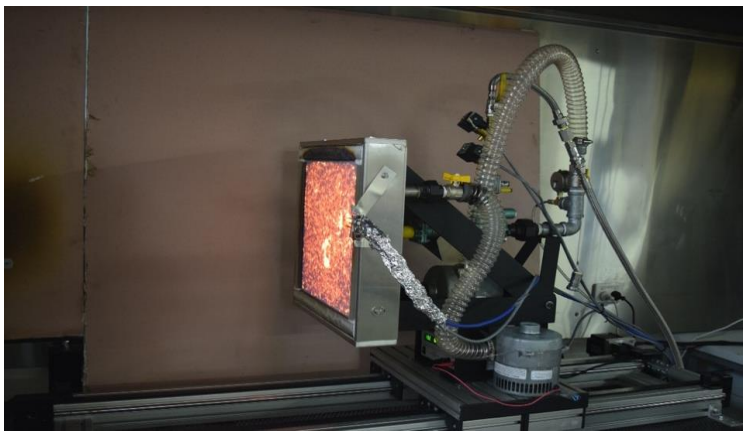

*Figure 3. 9: Radiant Heat panel in function.*

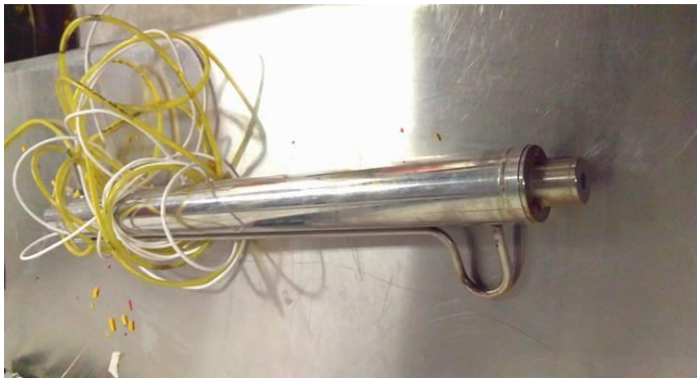

*Figure 3. 10: Water Cooled Schimdt-Boetler.*

Calibration of the H-TRIS was required in order to control the incident heat flux that was imposed on the surface of the protected steel plates. The calibration consisted of different steps and was repeated three times to have assurance of the incident heat flux imposed. The calibration of the H-TRIS was done using water cooled Schmidt-Boelter heat flux gauge (Figure 3.11) that was mounted at the gauge holder (Figure 3.15), the gauge and the gauge holder both were placed at the centre of the space at the back of the sample holder frame that's facing the radiant panel (Figure 3.8).

The position of the radiant panel was automatically positioned along the path of the linear motion system, the radiant panel moves from minimum to maximum distances with reference to the specimen location that was assigned by measuring the maximum and minimum distances from the surface of the gauge. To have assurance of the calibrations, three calibrations were done with different minimum and maximum distances, the readings were used then to generate calibration curves of incident heat fluxes vs. distance from the radiant panel as shown in Figure 3.12. Calibrations can be repeated anytime to account for different conditions which allows high number of repeatability.

*Figure 3. 11: Heat Flux gauge mounted on the gauge holder.*

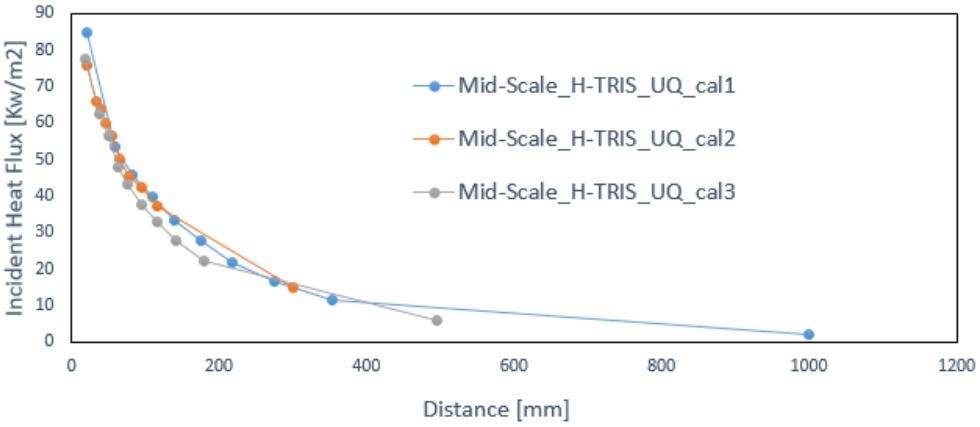


*Figure 3. 12: Plot showing incident radiant heat flux for different relative distances between the radiant panel and the exposed target surface of the test sample.*

### 3.2.3 Sample holder and instrumentation

Insulation material (Rockwool) has been placed inside the sample holder frame as presented in below Figure 3.13. The main aim of the insulation is trying to minimize heat losses at the lateral and back sides (unexposed parts) of the protected steel plates as low as possible. Insulation was placed in between the cavity in the sample holder frame to make sure that no air contact is between the back of the plate and the thermocouples.

Three thermocouples were attached to the protected steel plate at the unexposed side at different levels in order to see if there is variation in the steel temperature along the height of the steel plate, also in case of any malfunction of one thermocouple the others can compensate. Thermocouples were covered by aluminium tape and attached rigidly to the back of the steel plate, the unexposed side of the steel plate is assumed to be adiabatic as mentioned earlier. In addition, insulation was placed around the H-TRIS to make sure heat doesn't affect any surroundings.

*Figure 3. 13: Rockwool insulation filling the gap inside the sample holder.*

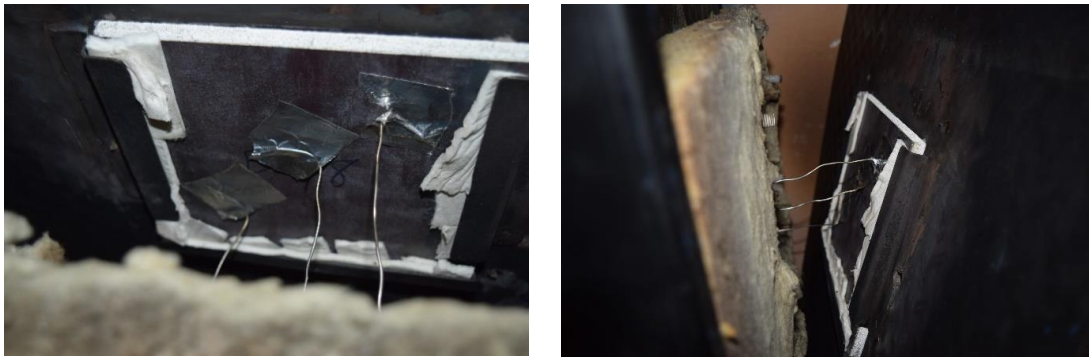

*Figure 3. 14: Thermocouples attached at the back side of the test sample.*

### 3.2.4 High resolution photo and video cameras

In order to track the expansion of the thin intumescent coating, two different still camera and video cameras were used. The Still camera was used at the side view of the sample holder aligned with the level of the thin intumescent coating so to have a lateral view of the coating when it's swelling, the still camera was taking photos every 30 seconds during the whole duration of the experiment (30 minutes). The other video camera was used in order to have a front view of the of the expansion process and to verify the shootings from the still camera. The still camera was not used for all tests, it was used for a specific set of tests that will be explained later in this section. In addition, to have better lighting during the experiments, two different stand LED lights were used and were positioned in different position ensuring no shadow can be observed at the sample plate.

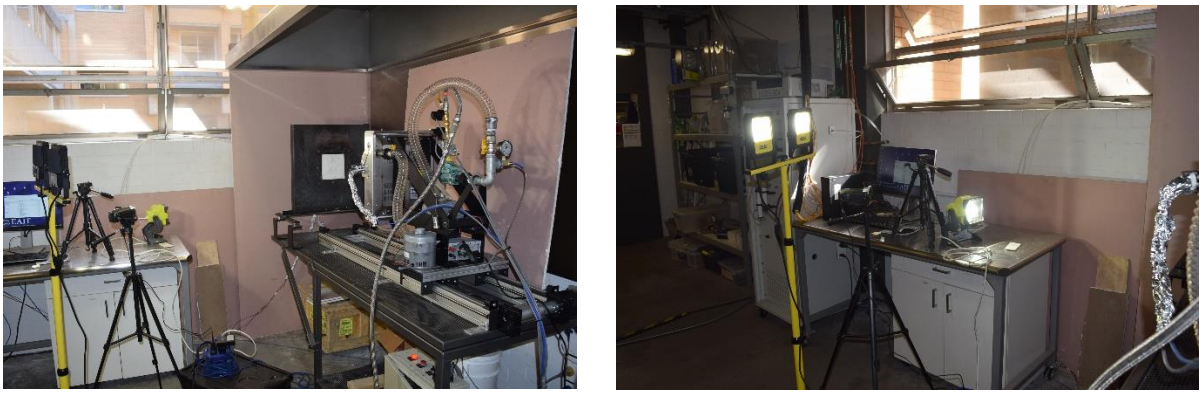

*Figure 3. 15: Cameras and LED Lights used in the tests.*

## 3.3 Test procedure

A total of nineteen tests were executed at varied levels of constant incident radiant heat fluxes. Table 3.3 shows the constant incident heat fluxes used during testing. Tests were performed in order to identify the occurrence of swelling activation under varied incident radiant heat fluxes. To achieve the abovementioned, three types of testing procedures were performed:

- Occurrence of swelling activation on protected steel samples;
- Test on unprotected steel samples; and
- Exploratory tests imposing stepwise heating increase.

### 3.3.1 Occurrence of swelling activation on protected steel samples

Table 3.3 shows the set of the tests used. It's worth highlighting that the reference system for the work shown herein indicates constant incident heat flux during testing and sample repetition; e.g. HF_50_1 indicates Sample #1 exposed to an incident heat flux of 50 kW/m$^2$.


*Figure 3. 16: Steel ruler used at the side to monitor the expansion.*

*Table 3. 3: Occurrence of swelling activation tests part.*

| Test Label | Incident heat flux Imposed. (Kw/m$^2$) | Dry Film Thickness (DFTs) (mm) | Still Camera Used |
|---|---|---|---|
| HF_50_1 | 50 | 1.57 | NO |
| HF_50_2 | 50 | 1.62 | YES |
| HF_40_1 | 40 | 1.44 | NO |
| HF_40_2 | 40 | 1.54 | YES |
| HF_40_3 | 40 | 1.62 | YES |
| HF_35_1 | 35 | 1.50 | NO |
| HF_35_2 | 35 | 1.55 | YES |
| HF_35_3 | 35 | 1.56 | YES |
| HF_27 | 27 | 1.48 | NO |
| HF_25_1 | 25 | 1.31 | YES |
| HF_25_2 | 25 | 1.45 | YES |
| HF_23_1 | 23 | 1.43 | YES |
| HF_23_2 | 23 | 1.38 | YES |
| HF_20 | 20 | 1.47 | NO |
| HF_16 | 16 | 1.51 | NO |

### 3.3.2 Test on unprotected steel samples

Beside the above listed tests, two tests were done on unprotected steel plate in order to see the effectiveness of the thin intumescent coating in general, the two heat fluxes used for the unprotected steel plates used were 35 and 50 Kw/$m^2$.

### 3.3.3 Exploratory tests imposing stepwise heating increase

In addition, two exploratory tests have been done using two different heat fluxes at two different durations during the tests, the first 15 minutes' duration used 20 Kw/$m^2$ and the other 15 minutes used 50 kw/$m^2$. Figure 3.17 gives better idea of these exploratory tests that could be used for future work recommendation.

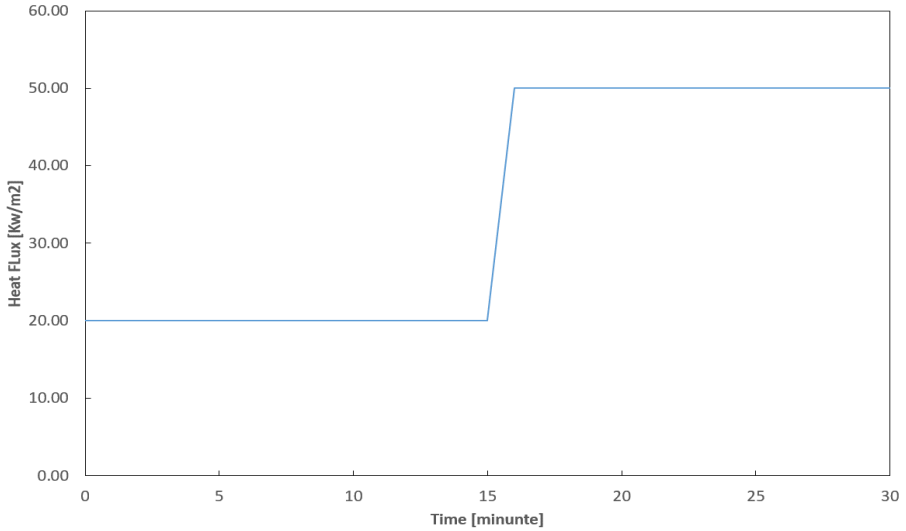


*Figure 3. 17: Exploratory stepwise heating increase curve.*

# 4. Results

In this section, results from the tests done throughout this work are described. This section is divided in three parts:

- Tests on protected steel samples,
- Tests on unprotected steel samples; and
- Exploratory tests imposing stepwise heating increase.

The results are presented describing visual observations of the swelling activation, rate of swelling and temperature of the steel.

## 4.1 Tests on Protected steel samples:

The main focus of these tests is to understand the conditions (time of exposure to incident heat flux and temperature of the steel) that governs the moment of the swelling activation.

### 4.1.1 Swelling activation

Within the scope of this work, swelling activation is described as **discrete swelling** or **total swelling.**

***Discrete swelling-*** when exposed to heat, intumescent coating undergo several chemical processes that were described in the literature review [section 2.3.3]. Discrete swelling is defined as the moment in when discrete and discrete swelling spots (referring to Figure 4.1) appear at the exposed surface of the tests samples. Depends on the heating conditions, discrete swelling spots may vary in size and time onsets. Figures below shows discrete activation spots for some of the tested samples.

*Figure 4. 1: Discrete swelling activation spots [HF_35_2] [7:30 minutes], [HF_25_1] [11 minutes] and [HF_16][21 minutes].*

Figure 4.2 shows the time that took for the discrete swelling spots to become notable at the exposed surface of the test samples. It's clear that higher heat fluxes lead to faster appearance of discrete swelling spots which lead to total swelling.

***Total swelling-*** One of the key challenges is to define the moment of total swelling, and state whether a specific sample under exposure of a specific heat flux experiences activation of the coating or not. The set of tests (refer to Table 3.3 in the Methodology section) indicated swelling rate under a range of heating fluxes and it also indicated the expansion curves for the tested samples which was a key factor to identify the total swelling activation.

Also, a numerous tests were executed to identify the critical incident heat flux that represented the threshold for total swelling activation. The procedure taken involved starting with high imposed

incident heat flux and gradually reduce the level of heat flux for following tests. This was done until no total swelling activation occurred; a series of repeated tests were performed for assurance.

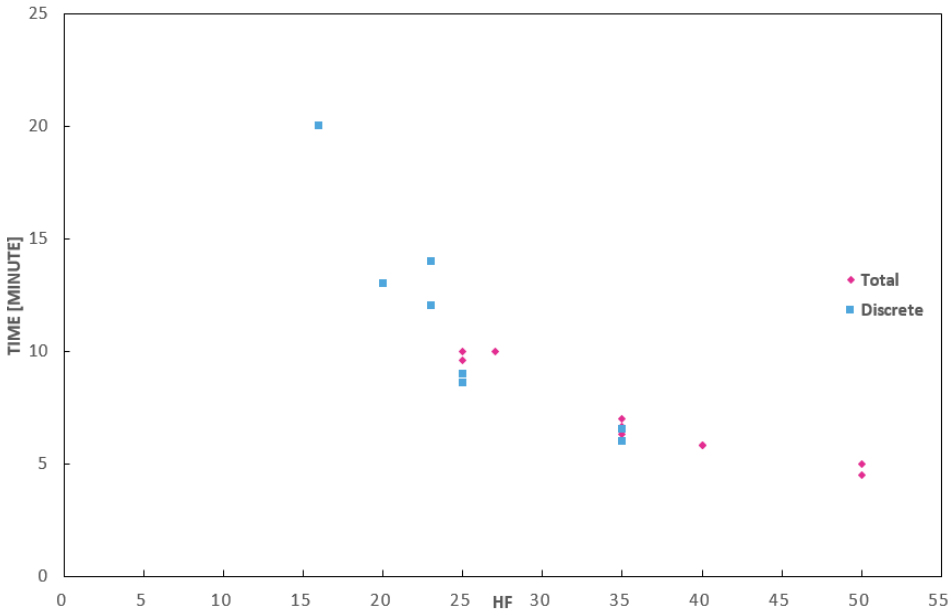


*Figure 4. 2: Total and discrete activation swelling time*

*Figure 4. 3: Total swelling activation, HF_35_2 [6:30 minute], HF_40_2 [6:48 minute] and HF_50_2 [4:30 minutes].*

Generally speaking, four different results were obtained from the tests. These tests helped defining the parameters for the total swelling activation:

1. Steel temperature;
2. Swelling rate;
3. Incident and net heat flux at the exposed surface; and
4. Accumulative net thermal energy flux at the exposed surface.

***Steel temperature-*** One of the most straight forward data was obtained by measuring the steel temperature, three thermocouples were positioned at the unexposed surface of the test sample. As little divergence was found from the thermocouple data, an average temperature was taken for each test. HF_35_2 steel temperature results as an example from one of the test is shown in figure 4.4.

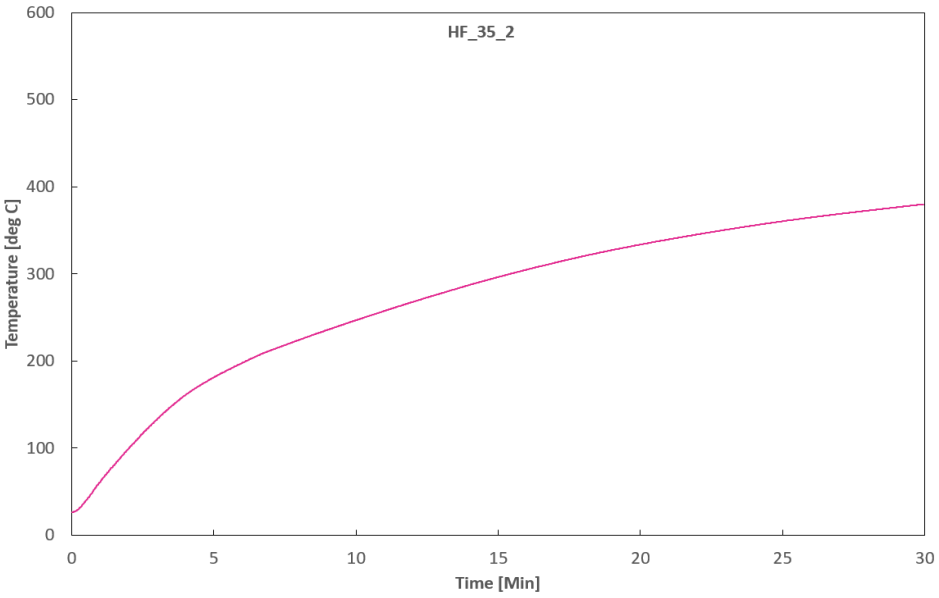


*Figure 4. 4: Steel temperature after 30 minutes of 35 Kw/m2 heat flux exposure.*

***Swelling rate-*** For the results from the still camera of the expansion curves are shown in Figure 4.5.

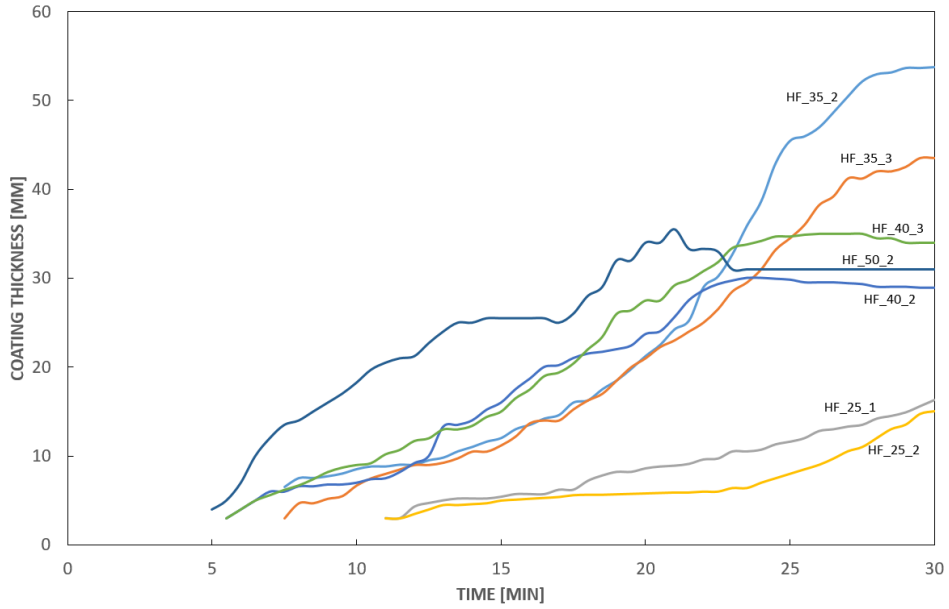


*Figure 4. 5: Intumescent Coating swelling curves obtained for each test.*

***Incident and net heat flux at the exposed surface-*** Incident heat flux controlled with the radiant panel distance relative to the sample's exposed surface was measured, and net heat flux as estimated from the heat transfer model are shown in Figure 4.6 for a sample exposed to a constant heat flux of 35 Kw/m$^2$. One of the key focus points from this heat transfer model is on the $q_{net}$ and $q_{inc}$. Recalling from section [3.1] that $q_{net}= q_{inc}- q_{loss}$. The following graph shows the results for $q_{net}$, $q_{inc}$ and $q_{loss}$ for 35 kw/m$^2$ as an example.

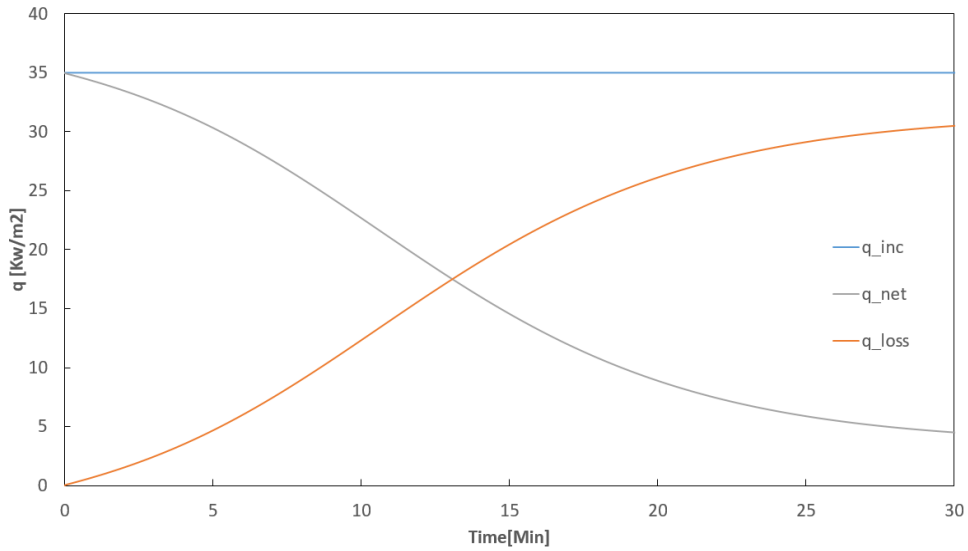


*Figure 4. 6: Heat transfer model results.*

***Accumulative net thermal energy flux at the exposed surface-*** calculating the area under $q_{net}$ is equal to the accumulative net thermal energy at the exposed surface of the test sample. It should be noticed that the area under the curve of $q_{net}$ is obtained based on a simple trapezoid calculation for the area under the curve. As a validation of the heat transfer model, a later section of this thesis shows the measured temperatures and the predicted ones from the heat transfer model are very close to each other. Figure 4.7 shows the net accumulative thermal energy flux for 35 Kw/m$^2$ as example as well.

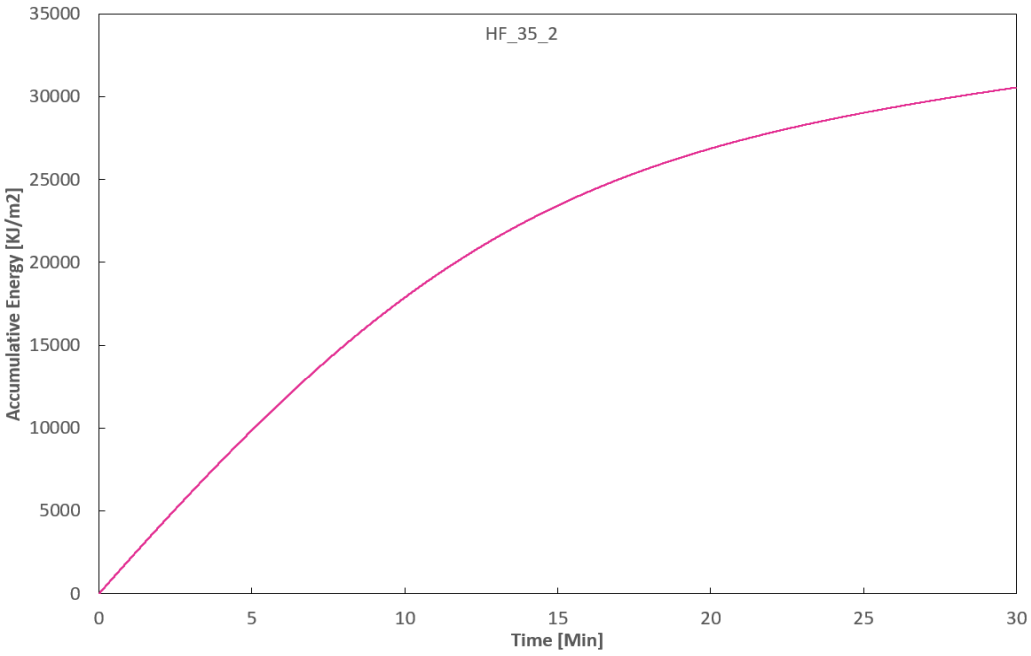


*Figure 4. 7: Accumulative net thermal energy flux under the onset curve.*

Analysis of these tests results up to the moment of swelling activation onset was done (refer to table 4.1). Figure 4.8 shows four test results plots combining all test data for a sample exposed to a constant incident heat flux of 35 kw/m$^2$. Equivalent plots for other tests are shown below, it should be highlighted that only the tests that have expansion curves are shown in these plots.

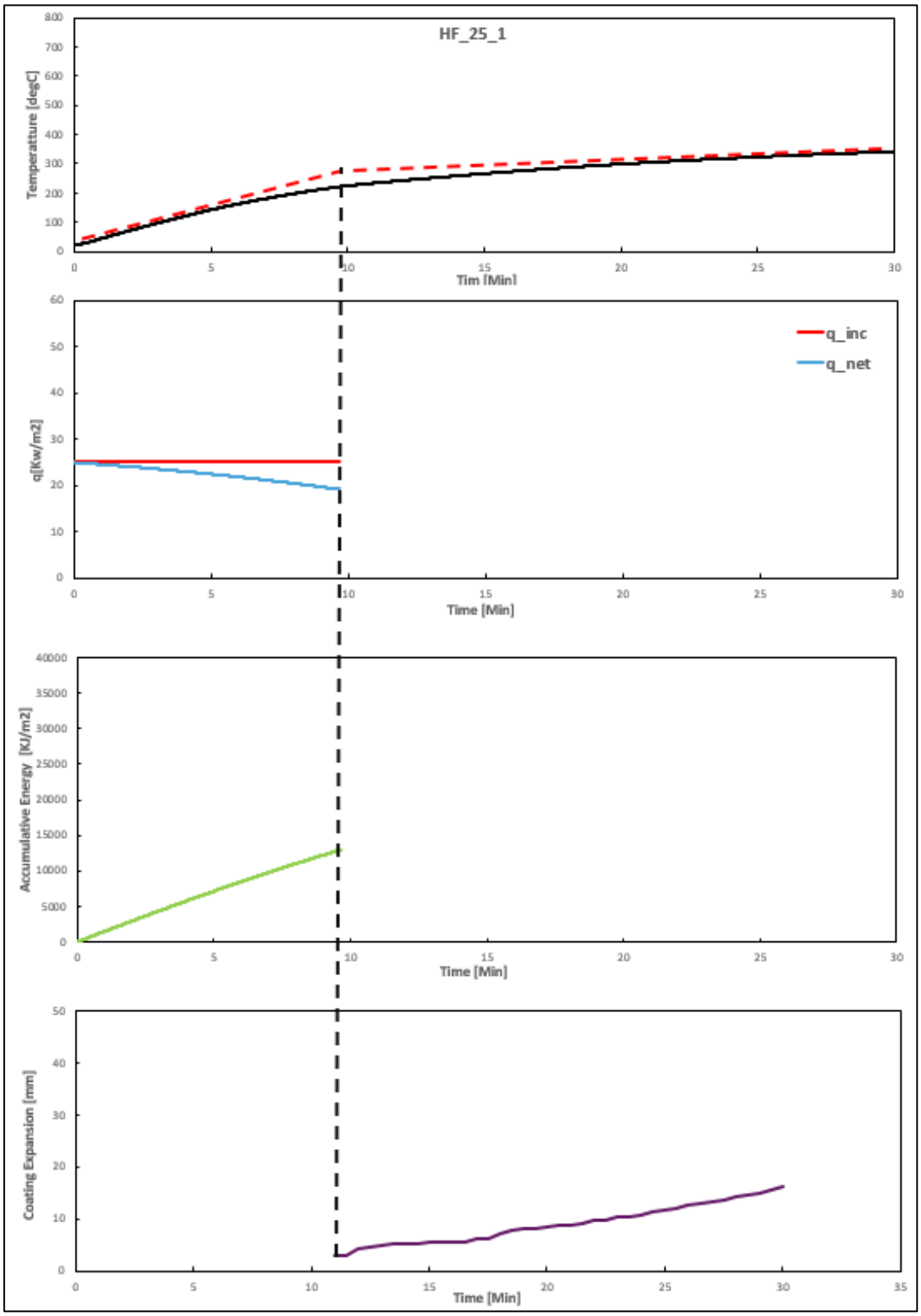


*Figure 4. 8: Test sample under constant incident heat flux at 25 kW/m2 (repetition #1).*

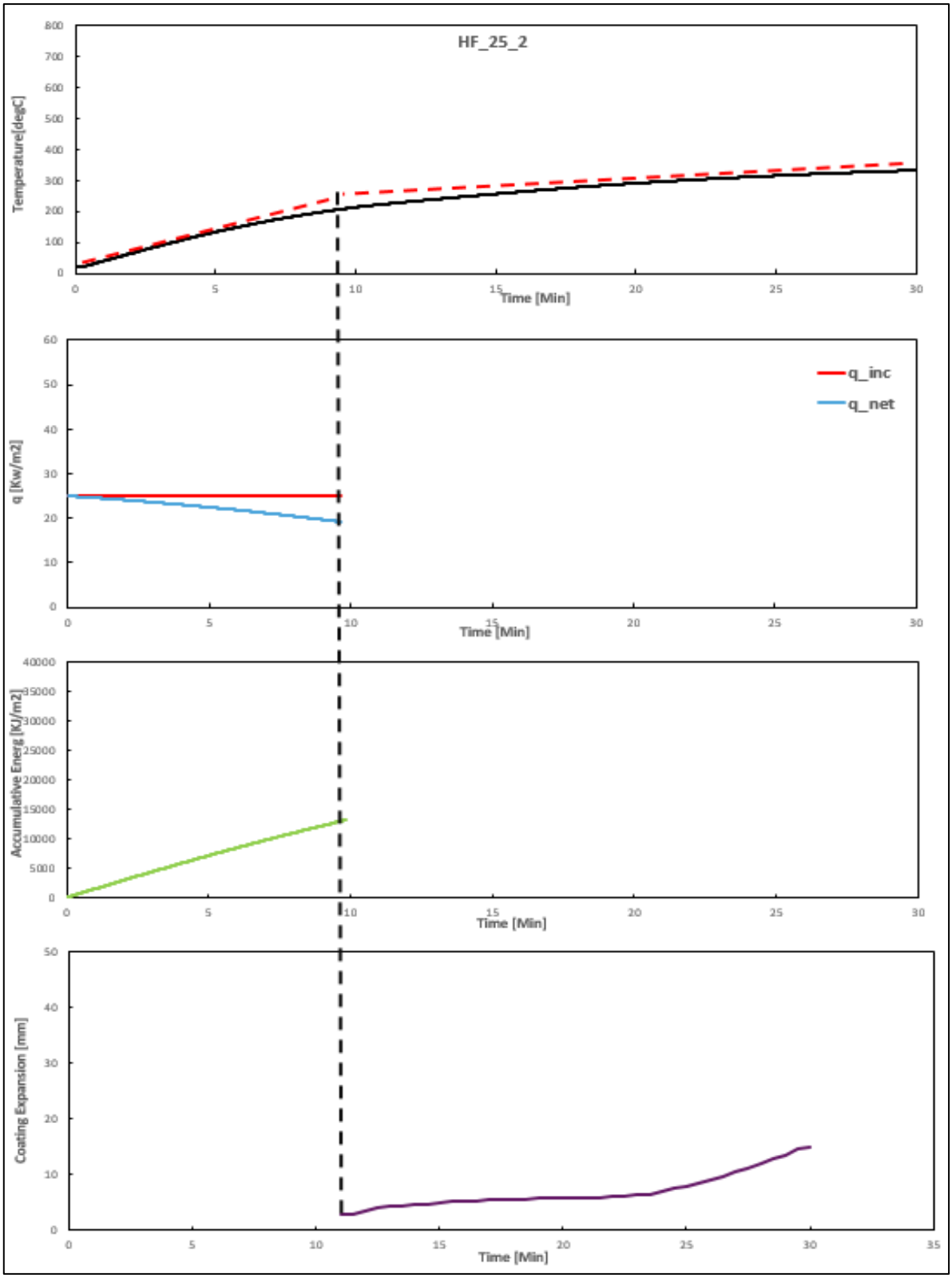


*Figure 4. 9: Test sample under constant incident heat flux at 25 kW/m2 (repetition #2*

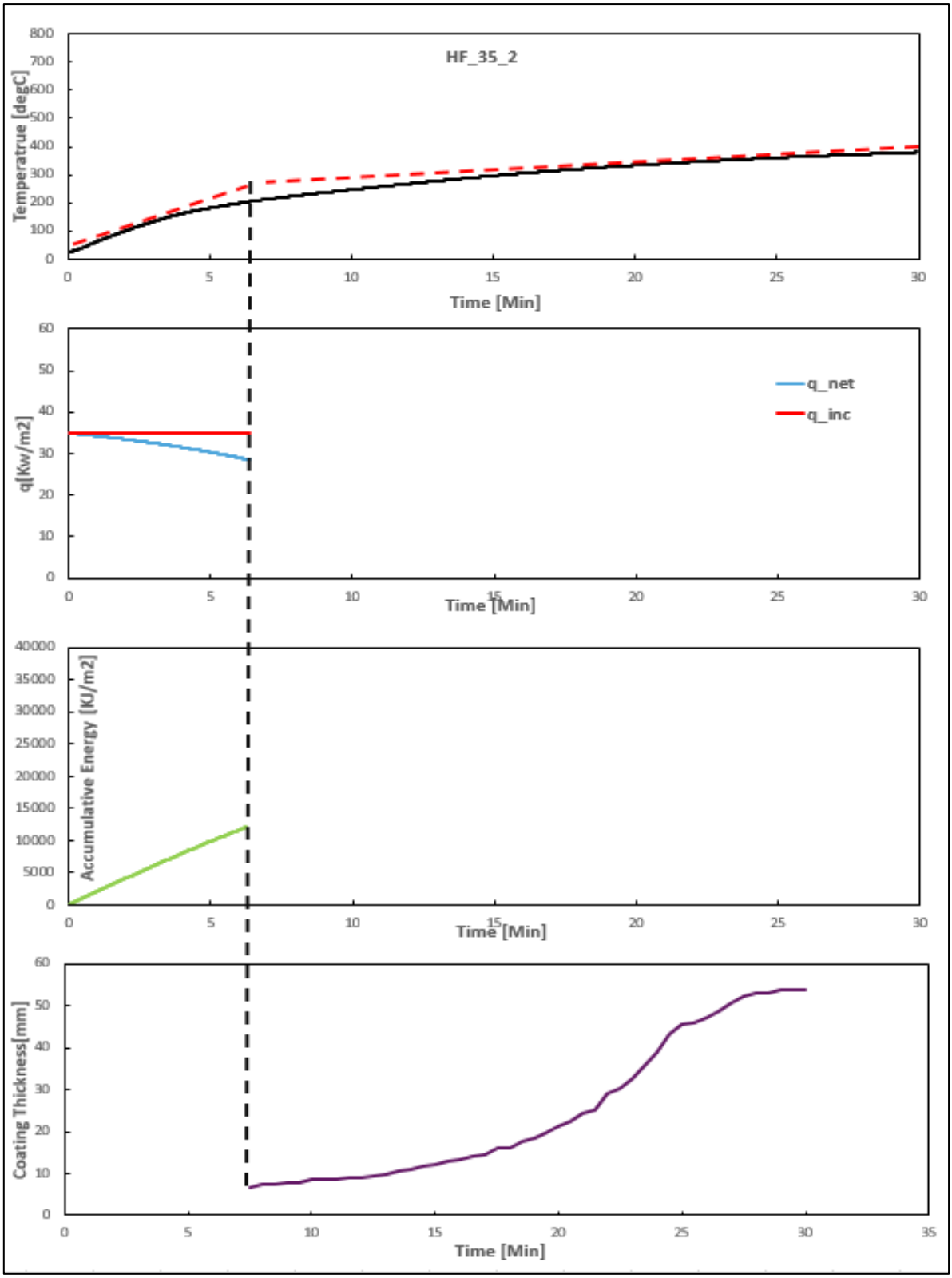


Figure 4. 10: Test sample under constant incident heat flux at 35 kW/m2 (repetition #2).

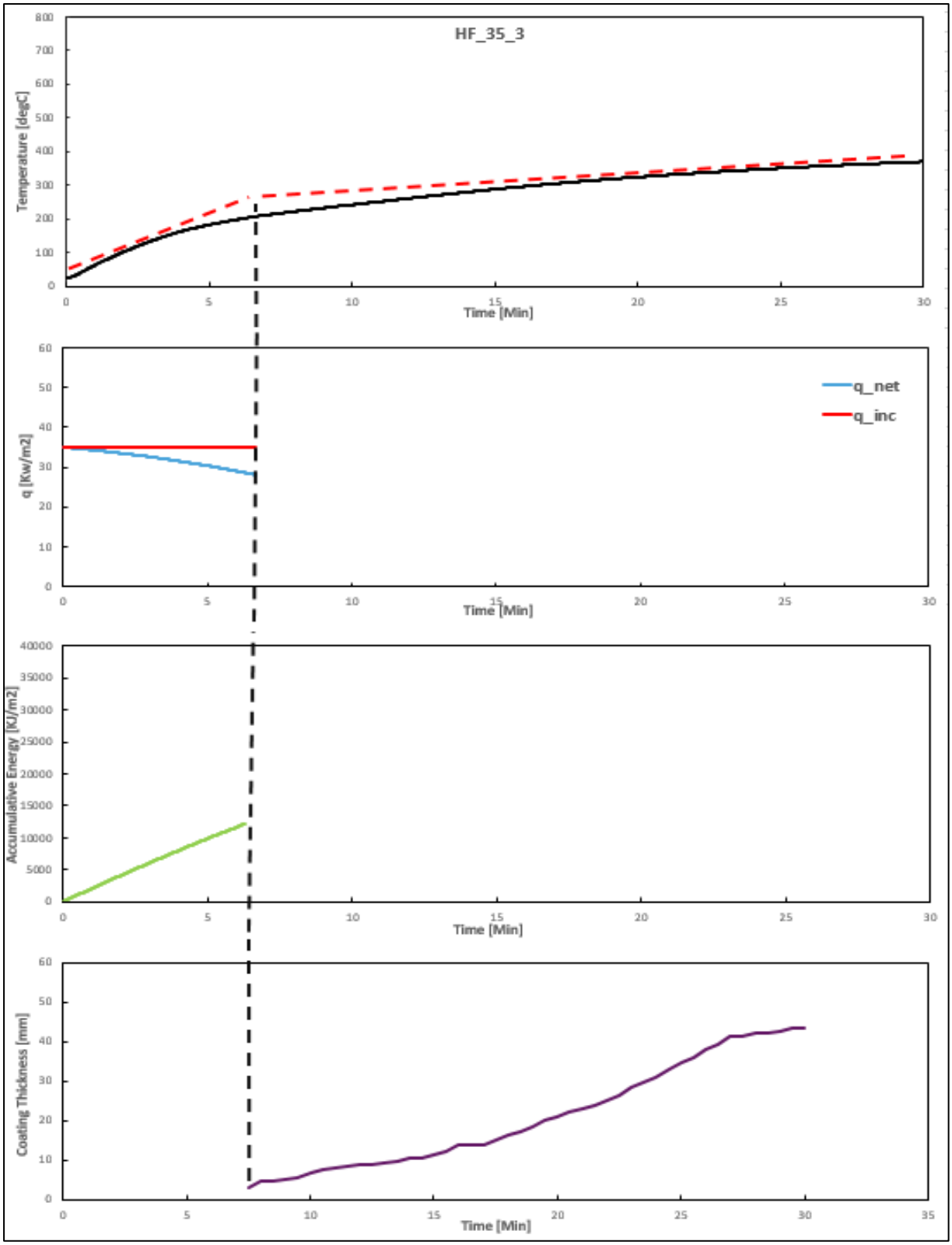


*Figure 4. 11: Test sample under constant incident heat flux at 35 kW/m2 (repetition #3).*

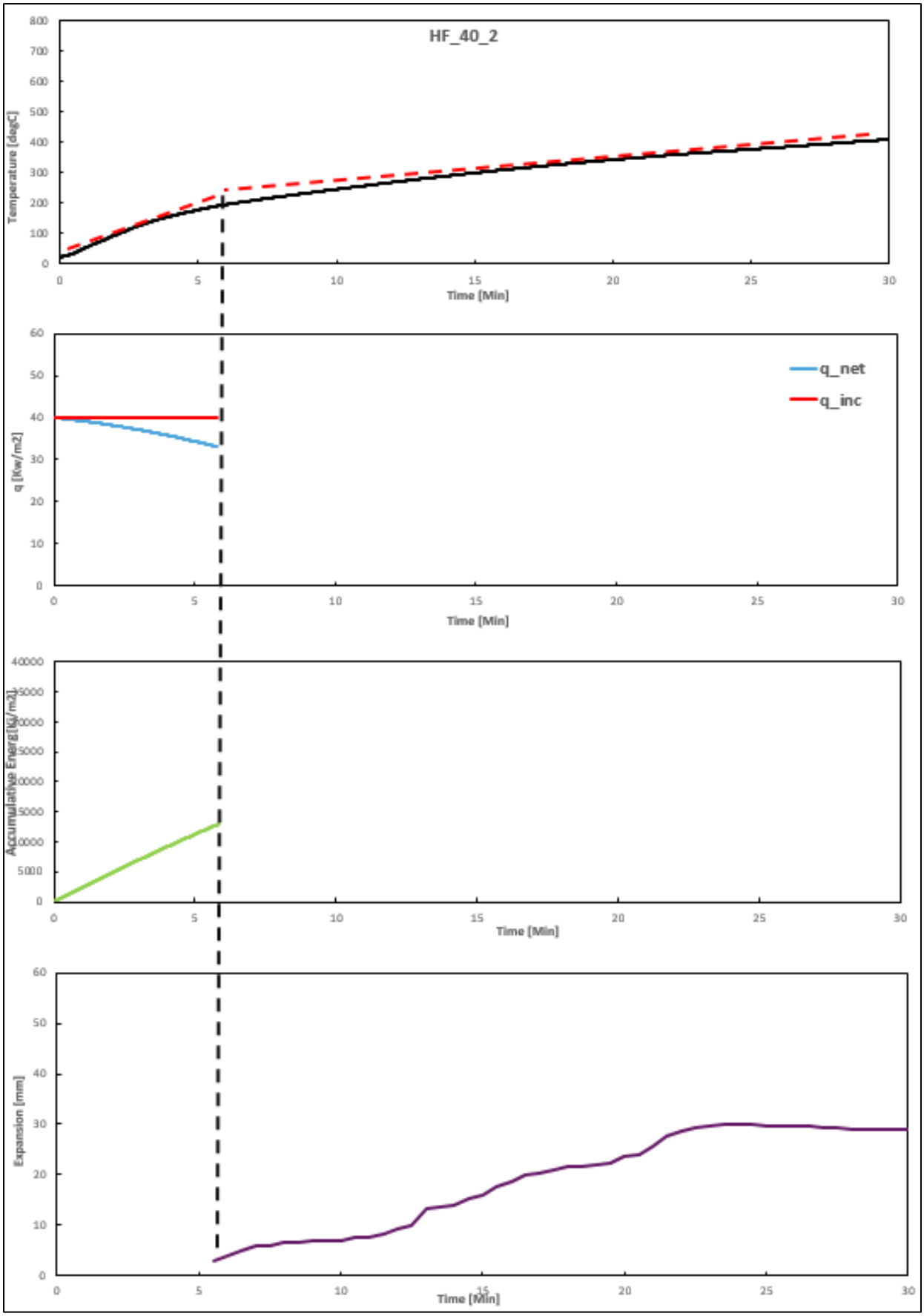


*Figure 4. 12: Test sample under constant incident heat flux at 40 kW/m2 (repetition #2).*

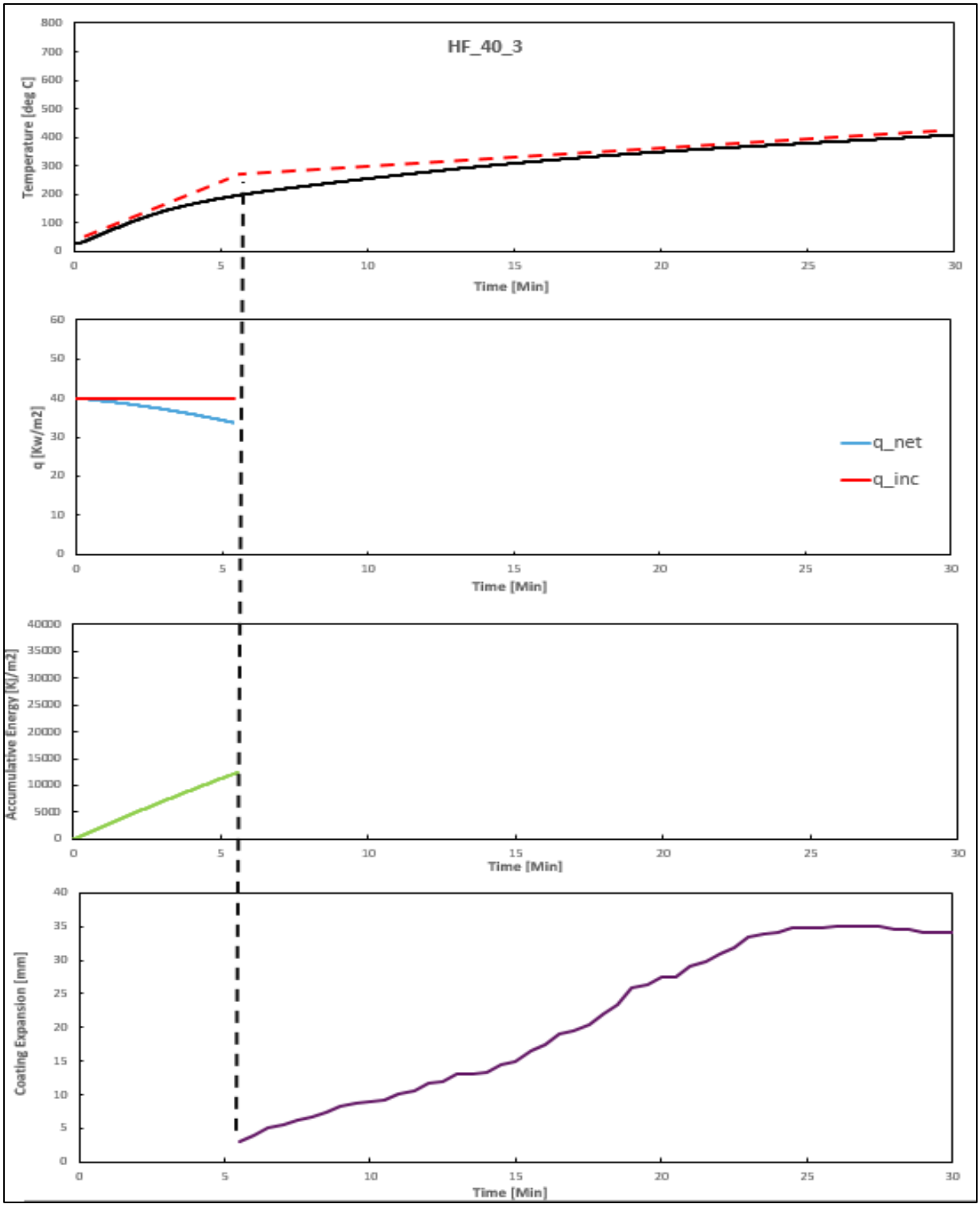


*Figure 4. 13: Test sample under constant incident heat flux at 40 kW/m2 (repetition #3).*

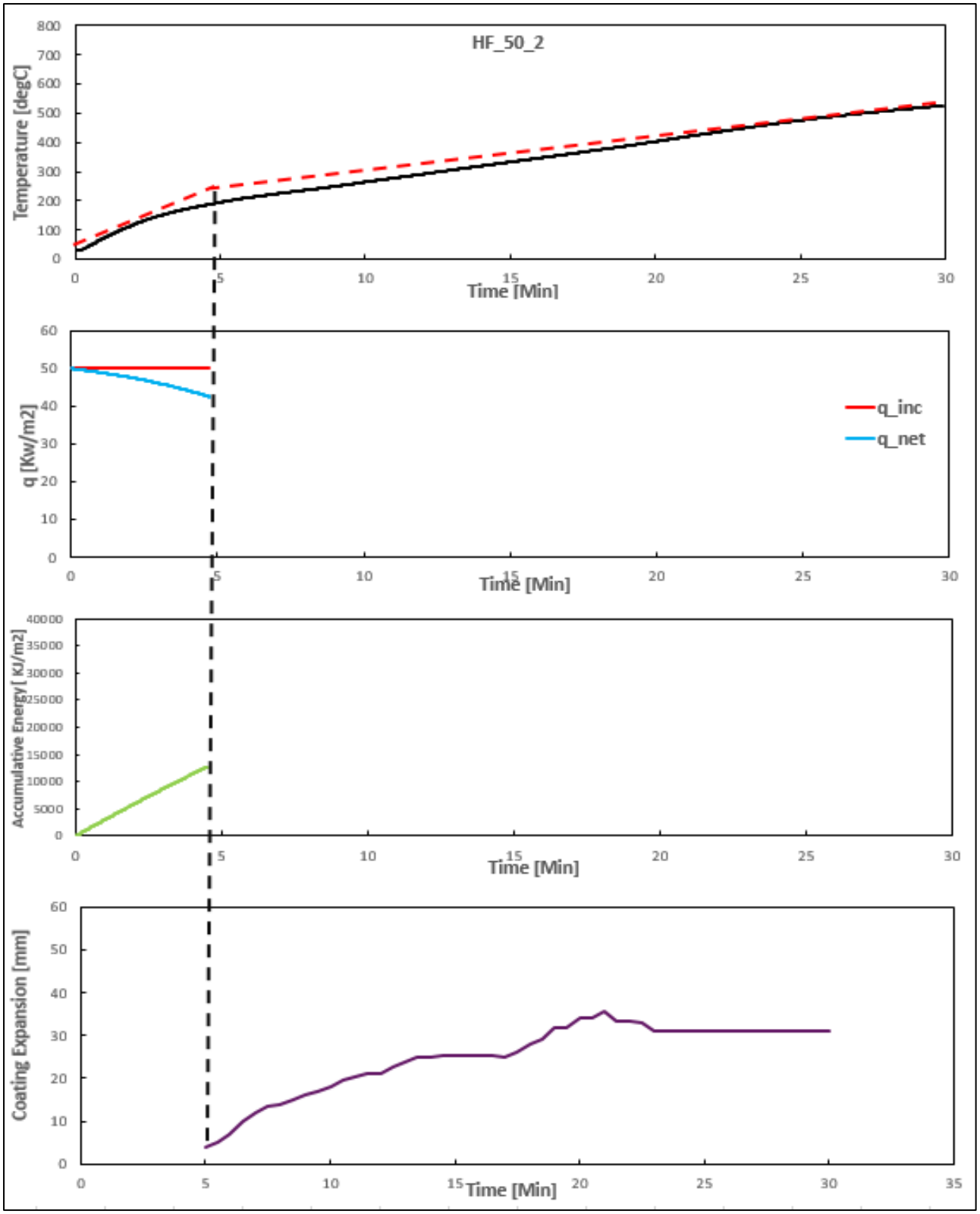


*Figure 4. 14: Test sample under constant incident heat flux at 50 kW/m2 (repetition #2).*

For top plots in the plots above, the dashed red lines are the tangent lines to the pre-activation and post-activation moments of the tests (when temperature increase is linearly increasing). Swelling activation was arbitrarily defined as the cross point of these tangent. This swelling activation onset time has been compared with the onset time from the still camera high resolution images and gave a good match. The combined graph for the other tests will be presented and discussed in the analysis and discussion section.

The following table shows the onset time for the different tests. It should be noted that HF_25, HF_23 and HF_16 didn't show adequate swelling when they were compared to others, a very little swelling occurred with very little expansion factor (refer to Figure 4.15) .It's worth mentioning that though swelling activation didn't occur but all of above mentioned tests have undergone discrete swelling activation spots described in the section earlier. Table 4.1 presents the time-swelling activation for each test performed within the scope of this work. As can be seen in Table 1, not all tests experienced activation.

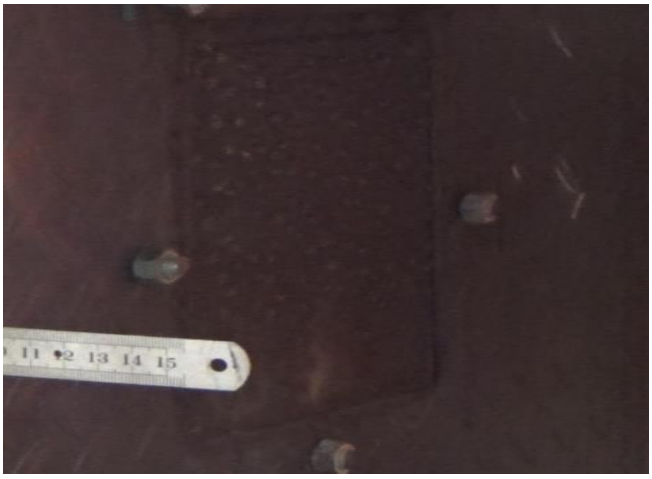


*Figure 4.* 15*: HF_16 surface appearance at 26 minutes of heat flux of 16 Kw/m2.*

*Table 4. 1: Activation details for the tests done in this work.*

| Test Label | Constant incident heat flux [kW/m²] | Successful total swelling | Time-to total swelling activation [min:sec] |
|---|---|---|---|
| HF_50_1 | 50 | YES | 5:00 |
| HF_50_2 | | | 4:30 |
| HF_40_1 | 40 | | (Activation time couldn't be found as the videos didn't exist) |
| HF_40_2 | | | 5:48 |
| HF_40_3 | | | 5:48 |
| HF_35_1 | 35 | | 7:00 |
| HF_35_2 | | | 6:19 |
| HF_35_3 | | | 6:40 |
| HF_27 | 27 | | 10:00 |
| HF_25_1 | 25 | | 9:34 |
| HF_25_2 | | | 10:00 |
| HF_23_1 | 23 | NO | n/a |
| HF_23_2 | | | n/a |
| HF_20 | 20 | | n/a |
| HF_16 | 16 | | n/a |

### 4.1.2 Swelling rate

This section describes the results obtained from the swelling behaviour of the thin intumescent coating, based on visual observation and data measured from the tests. Photos below show the intumescent coating after the occurrence of swelling from different tests, 30 min from the start of the test.

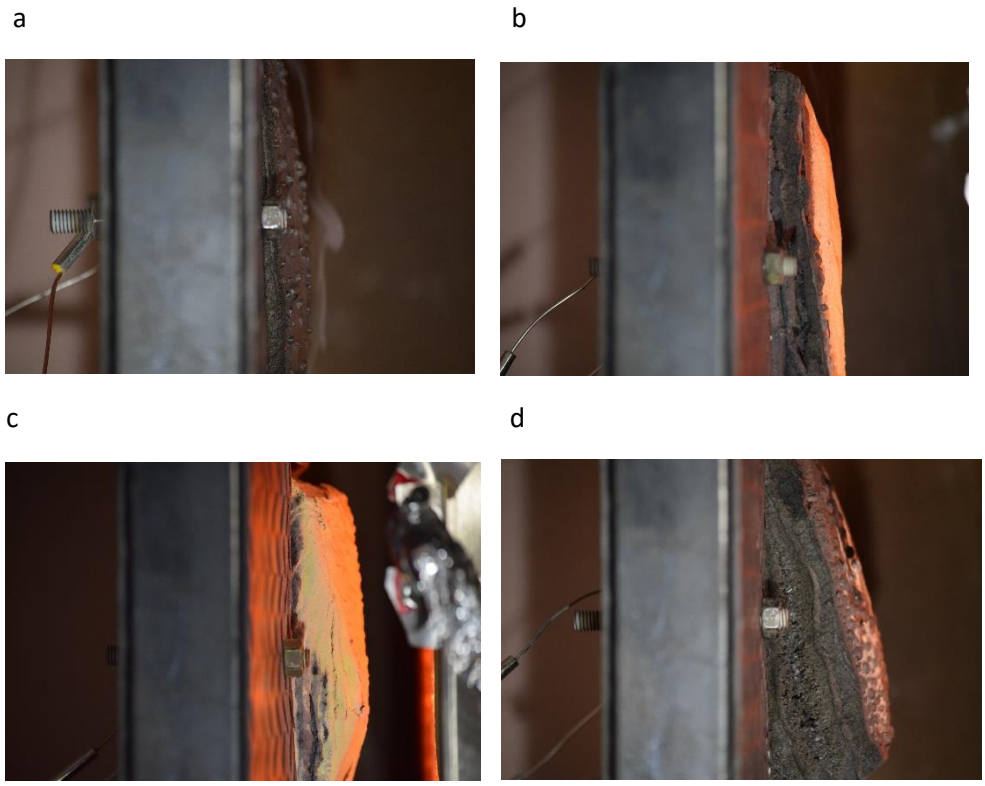


*Figure 4. 16: Total swelling activation after 30 minutes of exposure to different heat fluxes. (a) HF_25_2 (b) HF_40_2 (c) HF_50_2 (d) HF_35_2.*

Expansion measurements from the different tests are shown in Table 4.2 where the initial, final and the expansion factors are shown. The measurements of the final thickness has been checked twice by two different methods. The first one with steel millimetre ruler, 9 different points has been measured along the surface of the coating because it was noticed that one part of the coating didn't swell in the same rate as others (Figure 4.16) then an average value was taken to account for the final thickness of the coating. Figure 4.17 below shows nine different points that were measured throughout the surface of the coating.

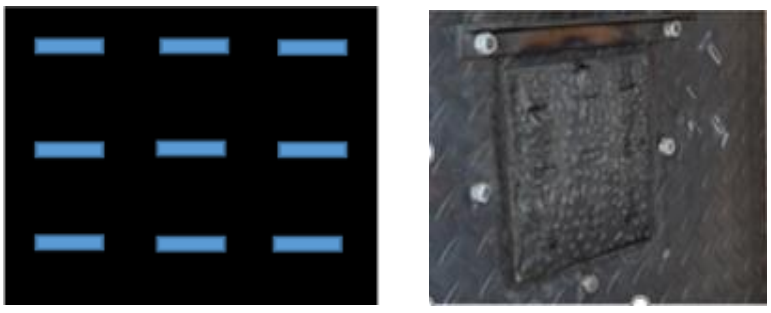

*Figure 4. 17: Nine different measuring points throughout the coating.*

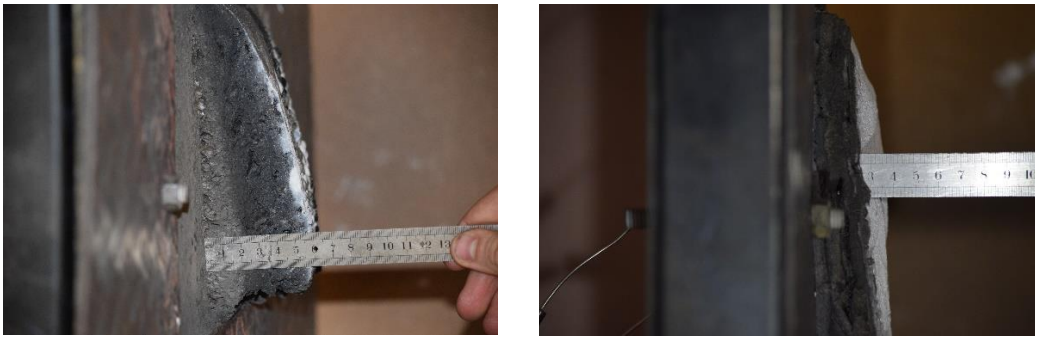

*Figure 4. 18: Using the steel millimetre ruler to measure the final thickness of the coating.*

The other method was to monitor the expansion every 30 seconds by the high resolution camera during the duration of the test, the photos has been analysed by using Adobe Photoshop and estimate the length of 1mm in terms of number of photo pixels. It's noticed there is a good matching between the readings from the camera and the final measurements from the steel ruler.

The measurements from the camera considered the expansion from the moment it was observed from the edge of the sample holder frame, 3 mm was the initial readings for the expansion curve for all the tests as this was distance between the surface of the coating and edge of the sample holder frame prior to swelling.

*Table 4.2: Initial DFT, final thickness and Swelling ratio from the different tests.*

| Test Number | Initial DFT | Final thickness | Swelling Ratio |
|---|---|---|---|
| HF_50_1 | 1.57 | 25.00 | 15.92 |
| HF_50_2 | 1.62 | 29.60 | 18.27 |
| HF_40_1 | 1.44 | 32.56 | 22.61 |
| HF_40_2 | 1.54 | 31.33 | 20.34 |
| HF_40_3 | 1.62 | 33.90 | 20.92 |
| HF_35_1 | 1.50 | 40.33 | 26.88 |
| HF_35_2 | 1.55 | 43.33 | 27.95 |
| HF_35_3 | 1.56 | 43.90 | 28.14 |
| HF_27 | 1.48 | 19.22 | 12.98 |
| HF_25_1 | 1.31 | 16.40 | 12.52 |
| HF_25_2 | 1.45 | 15.44 | 10.65 |

## 4.2 Tests on unprotected steel plates

Two tests as described earlier has been done on unprotected steel plates in order to have a better understanding of the onset of activation in terms of temperature results and understand the effectiveness of the thin intumescent coating on the steel temperature.

The two heat fluxes used were HF_35 and HF_50 Kw/m$^2$, the steel temperature was measured. The following graph shows the temperatures results from the steel plate for the both heat fluxes.

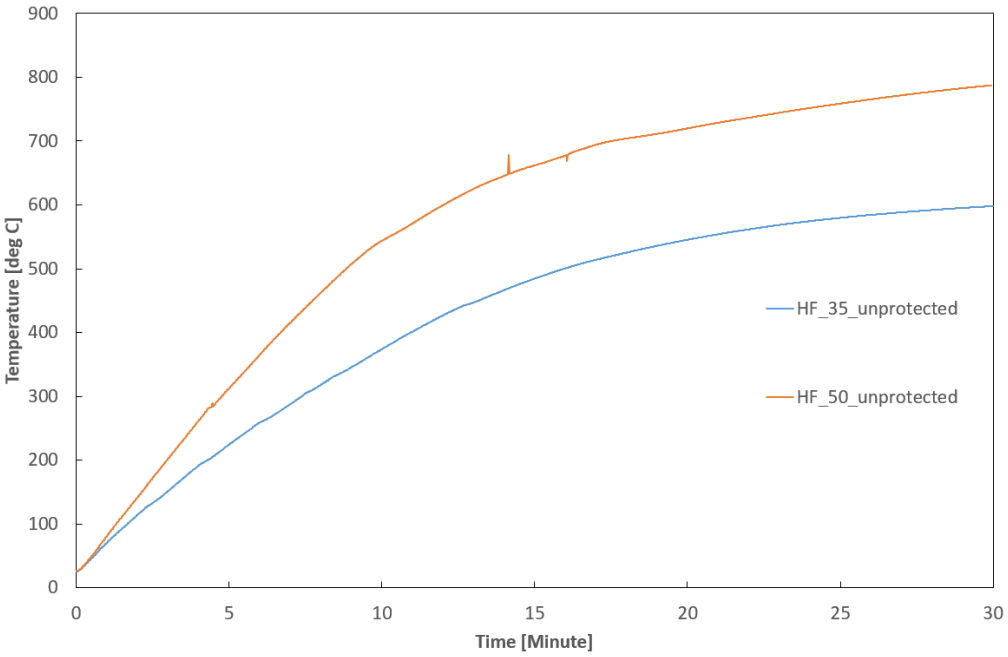


*Figure 4. 19: Unprotected steel temperatures after exposure to 30 minutes heat fluxes.*

## 4.3 Exploratory tests imposing stepwise heating increase

As explained earlier, two tests were performed using stepwise increase of incident radiant heat flux; for the first 15 minutes incident radiant heat flux was 20 Kw/m$^2$ and from then onwards, incident radiant heat flux was 50 kw/m$^2$ ( refer to Figure 3.16 ). Samples were instrumented in a similar way to prior tests. The aim of these tests is to understand the activation of the thin intumescent coating under a transient of heating condition and check that whether swelling activation is effective under these conditions. Swelling rate as measured for a stepwise heating increase is shown in Figure 4.21.

*Figure 4. 20: Intumescent coating after stepwise heating increase.*

It should be noted that the heating flux was not directly 50 Kw/m$^2$ at 15 minutes, the panel started moving closer to the surface of the sample prior to minute 15 which explains the reason behind the rapid increase of the coating thickness before 15 minutes. While for temperature readings the following result was obtained from these tests. For each test, the temperature and the swelling rates (if applicable) are shown below.

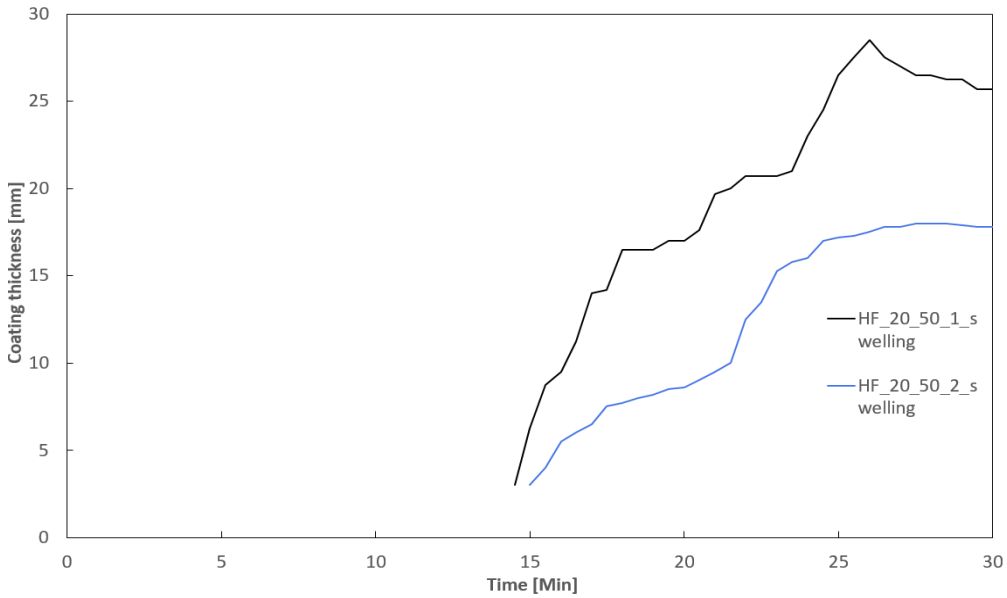


*Figure 4. 21: Expansion curve for stepwise heating increase.*

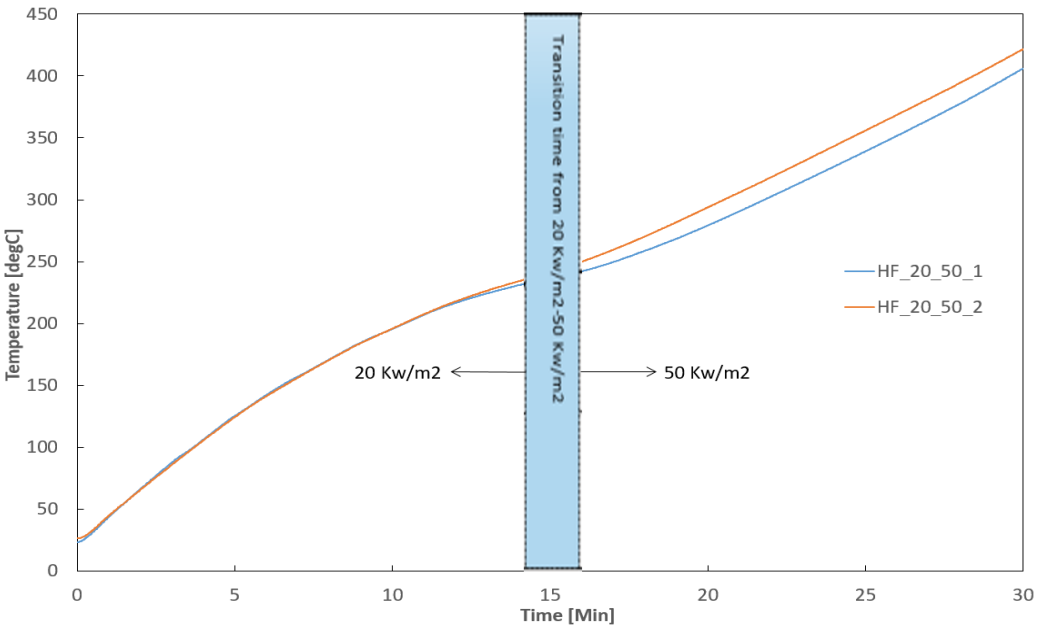


*Figure 4. 22: Temperature results for stepwise heating increase.*

For each test, the temperature and the swelling curves (if applicable) are shown below:

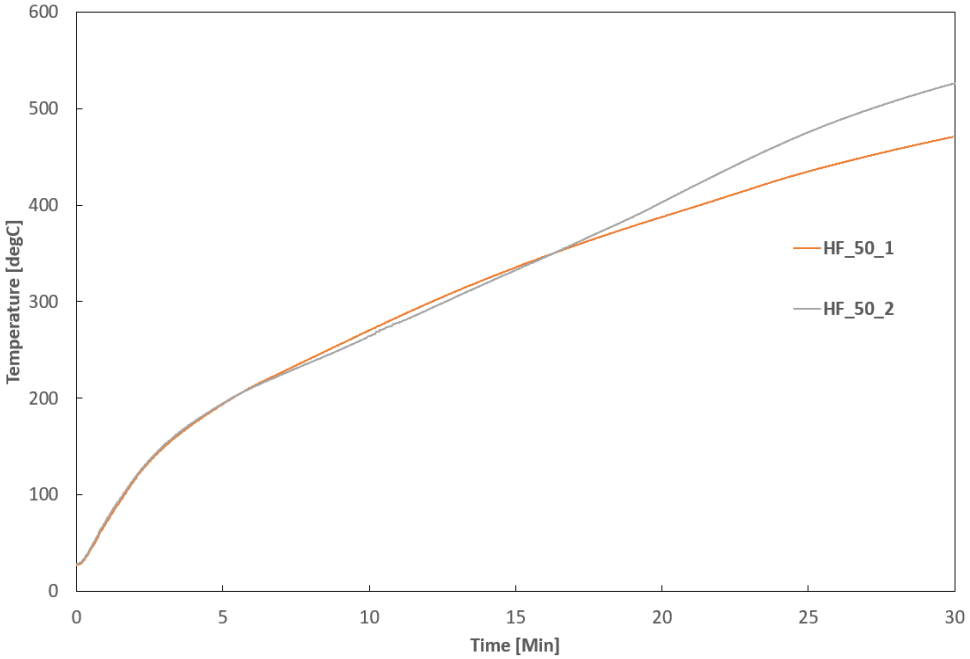


*Figure 4. 23:H_50 temperature curves.*

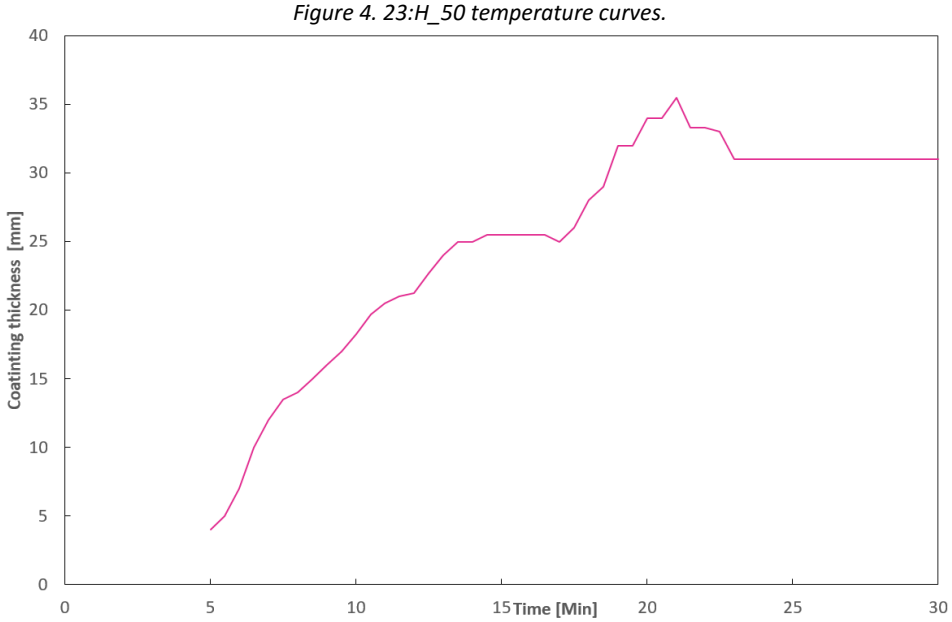


*Figure 4. 24:H_50_1 swelling rate curve.*

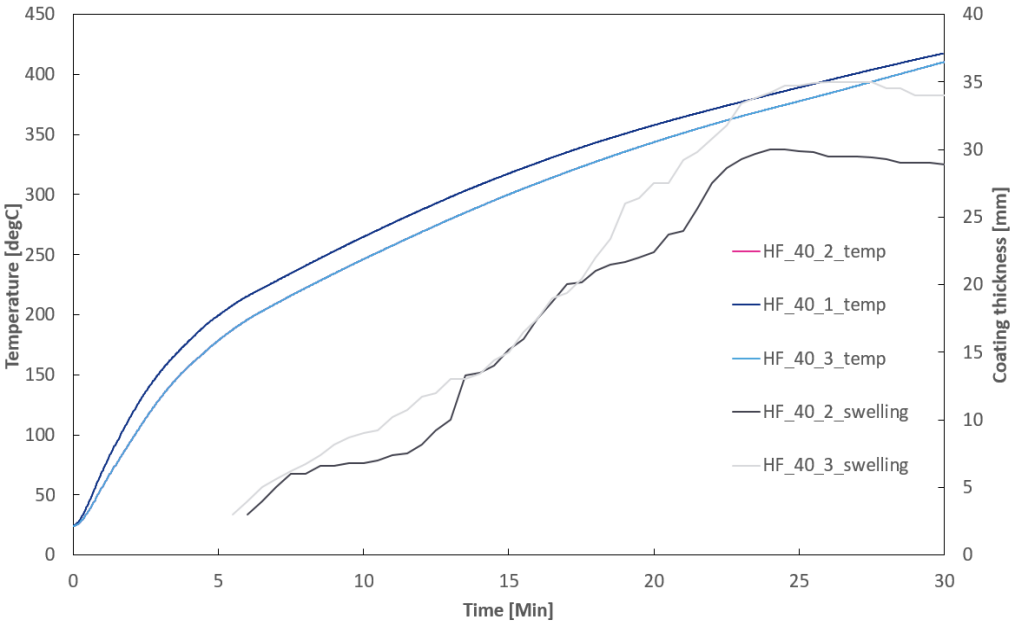


*Figure 4. 25: H_40 Temperature and swelling rate curves.*

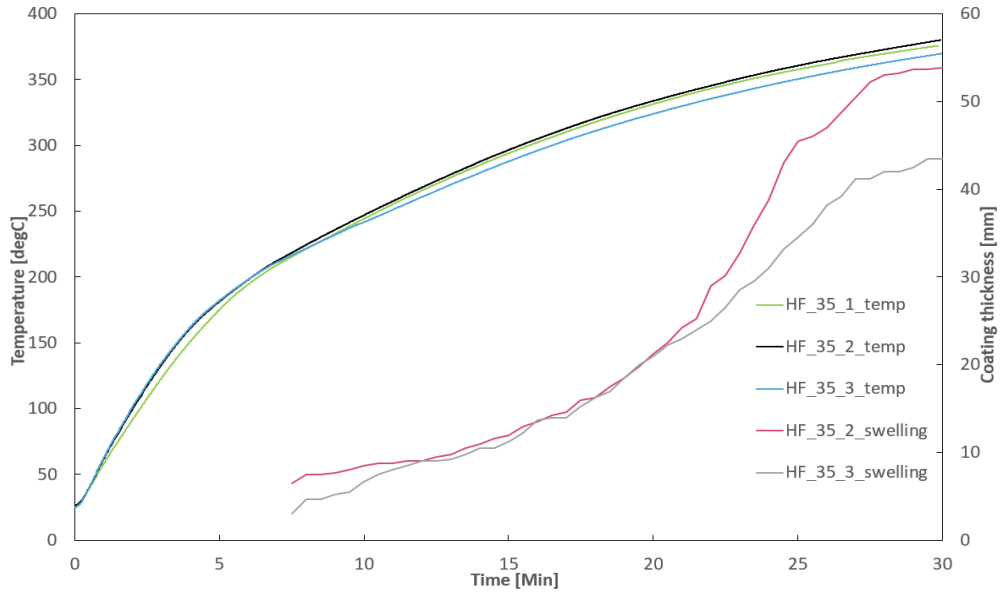


*Figure 4. 26: H_35 Temperature and swelling rate curves.*

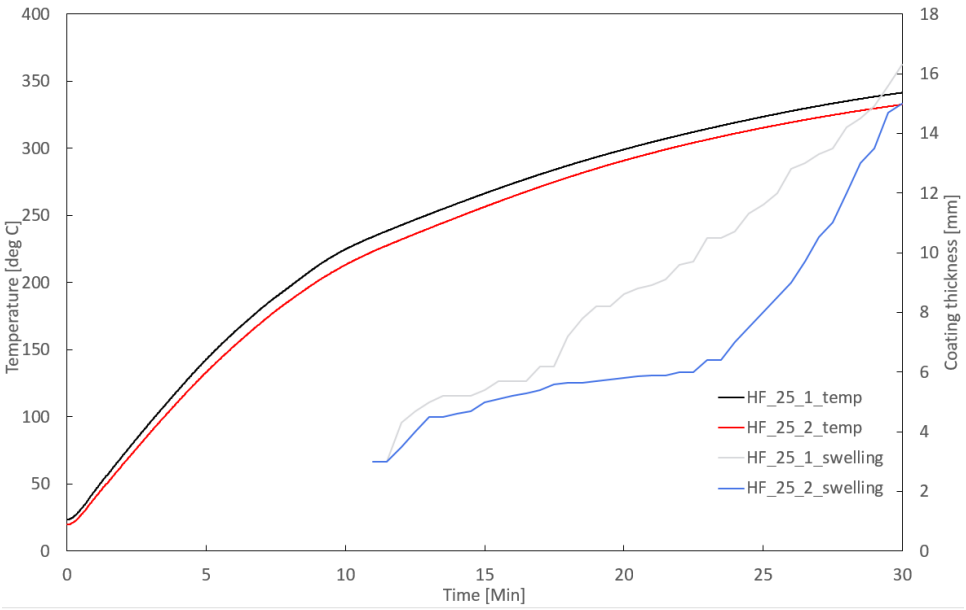


*Figure 4. 27: HF_25 temperature and swelling rate curves.*

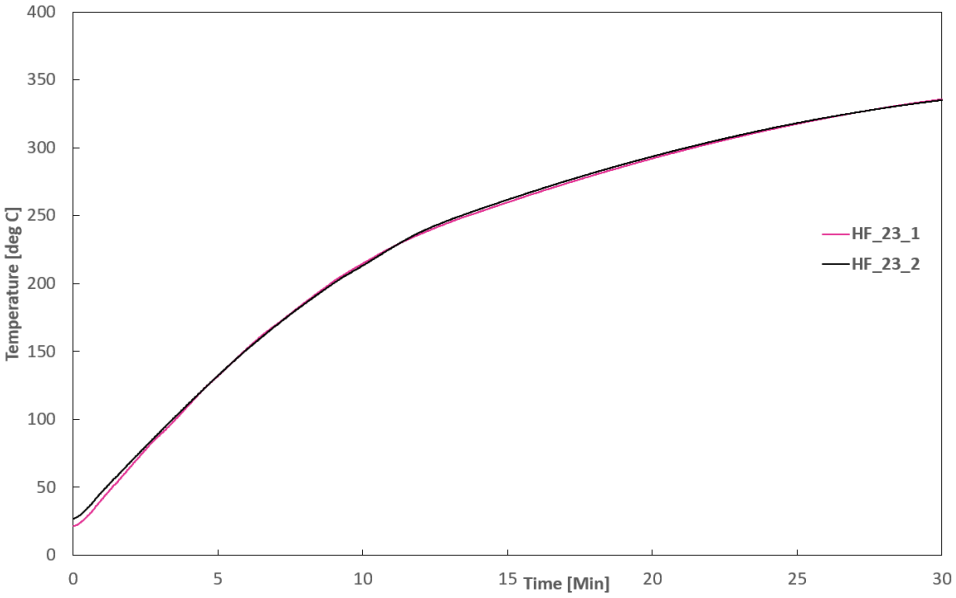


*Figure 4. 28: HF_23 Temperature curves.*

# 5. Discussion and analysis

In this section analysis and discussion of the results stated in the previous section will be presented. The focus will be on total swelling activation, tests on unprotected steel, and the exploratory work tests with stepwise heating increase. It should be highlighted that this is a novel study over the activation of the intumescent coating and therefore no literature review is available to compare with the results found here.

## 5.1 Total swelling activation

### 5.1.1 Analysis of steel temperature

One of the findings from the test results (refer Figures 4.8 to 4.14) is that the moment of the swelling activation can be identified by looking at steel temperature measured at the unexposed surface of the test samples; regardless of the heat flux imposed. It has been noticed that the back-steel temperatures for swelling activation happens for steel temperatures between 180 and 220 $^{o}$C. The following graph shows the back-steel temperature when the intumescent coating to start total swelling activation. *From now on the back-steel temperatures that was stated earlier will be referred to as "activation temperature" for the coating, more justification will follow.*

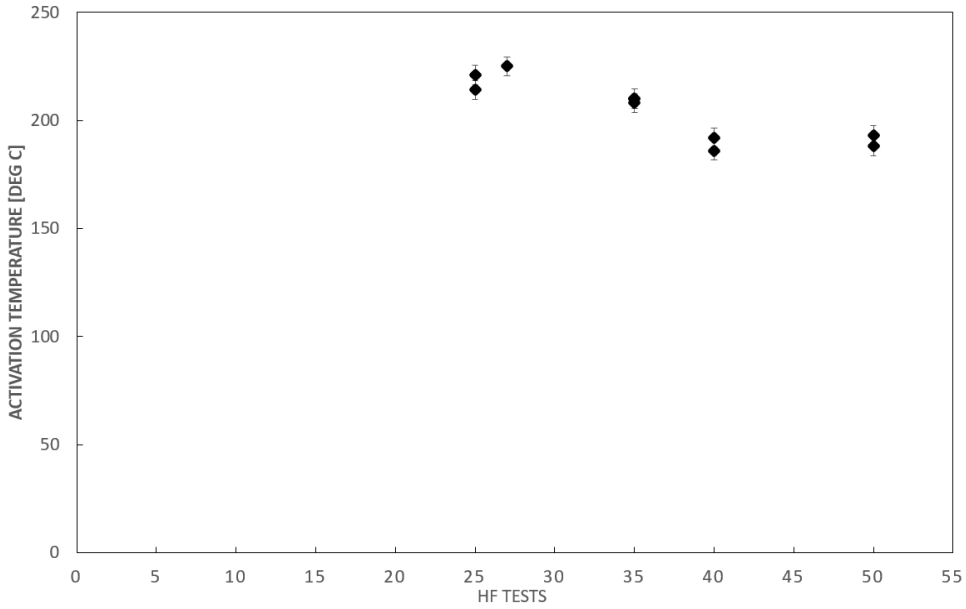


*Figure 5. 1: Temperature of the steel upon total swelling activation of the test sample*

It can be seen that it's possible to state that the coating under high heat fluxes requires a lower activation temperature (not necessarily) to reach the activation temperature for the swelling activation. HF_25 and HF_27 tests have the highest activation temperatures while HF_50_2 and HF_40_3 tests seem to be the lowest activation temperatures. It can be seen as well there is a very good matching between the repeated tests. In addition, there is a good matching between the temperature ranges mentioned in the literature [Section 2.3.3] compared to the ones found in this work. It can be stated as well that the critical heat flux for the swelling activation based on the back steel temperature analysis is within the range of 23 to 25 Kw/m$^2$. Frankly this a bit rough to state, as more tests has to be done to confirm this statement, but as have been presented in the result section and the analysis that has been done after, this can be generalised to state it's within this range.

Its indeed the back steel temperatures that have been used to locate the swelling activation for the coating but from the previous sections It was shown that both coating and steel are thermally thin at ambient temperatures, its assumed here that both steel and the coating will remain thermally thin until swelling activation takes place, more specific analysis has to be done to analyse the effective thermal conductivity of the coating at the swelling activation moment.

*It should be highlighted that HF_23, HF_20 and HF_16 tests all have reached this range of temperatures needed for swelling activation but none of them swelled, which can lead to a point that the activation of the thin intumescent coating activation is heat flux dependent not only a temperature dependent*

### 5.1.2 Analysis of accumulative thermal energy flux

The other results that were found from the studies that the swelling activation starts within a specific range of accumulative thermal energy flux as was shown the in the result section, this accumulative thermal energy flux needed for the swelling activation to start has been called “activation energy” in this work. It can be seen from the figure below that the activation energy falls within a small range of energy regardless of the heat flux value imposed but at the same time onset time for total swelling activation descends as the heat flux increases which can interpreted as that thin intumescent coating is heat flux dependent not only a temperature dependent.

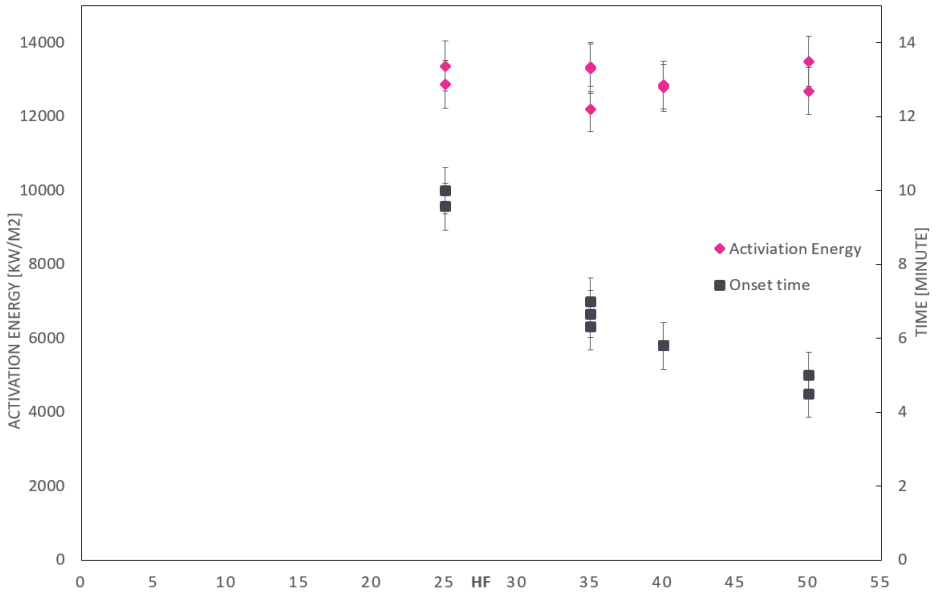


*Figure 5. 2: Comparison between activation energy and onset time.*

The same comparison has been done between the activation energy and activation temperature as shown in the following figure. It can be seen as well that the coating under high heat fluxes requires less activation temperatures and similar activation energy to activate compared when it’s exposed to less heat fluxes. It can be seen as well that there is a good comparison and matching between the repeated tests.

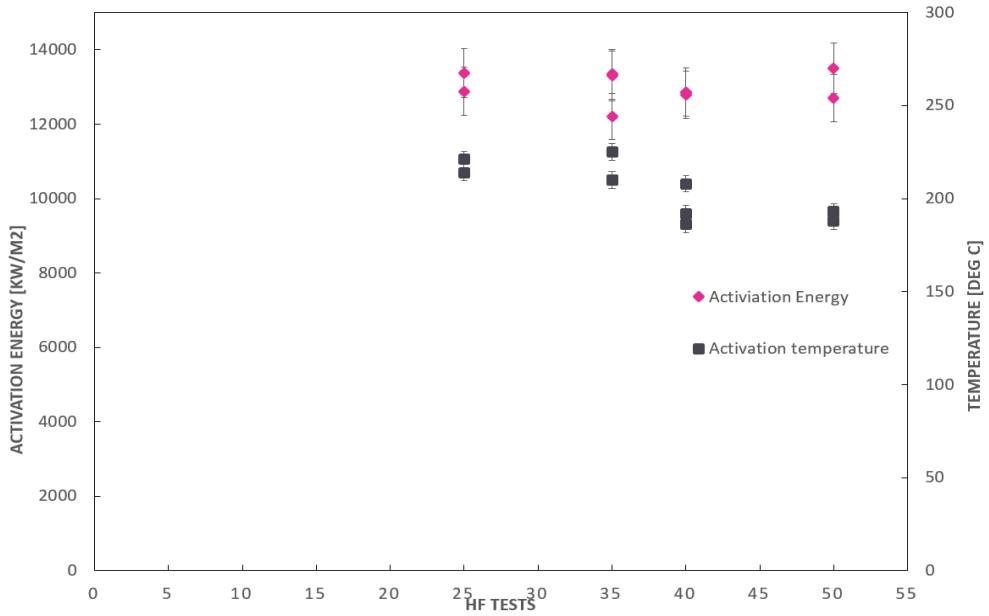


*Figure 5. 3: Comparison between activation temperature and activation energy.*

### 5.1.3 Analysis of discrete and total swelling

For HF_35 and HF_25 tests, it has been mentioned that both has been undergoing a local activation points before transitioning to global activation throughout the surface. The time difference between the start of the local activation points and the start of the global activation is shown in the below Figure. It can be seen that HF_35 developed into global activation slightly faster than HF_25.

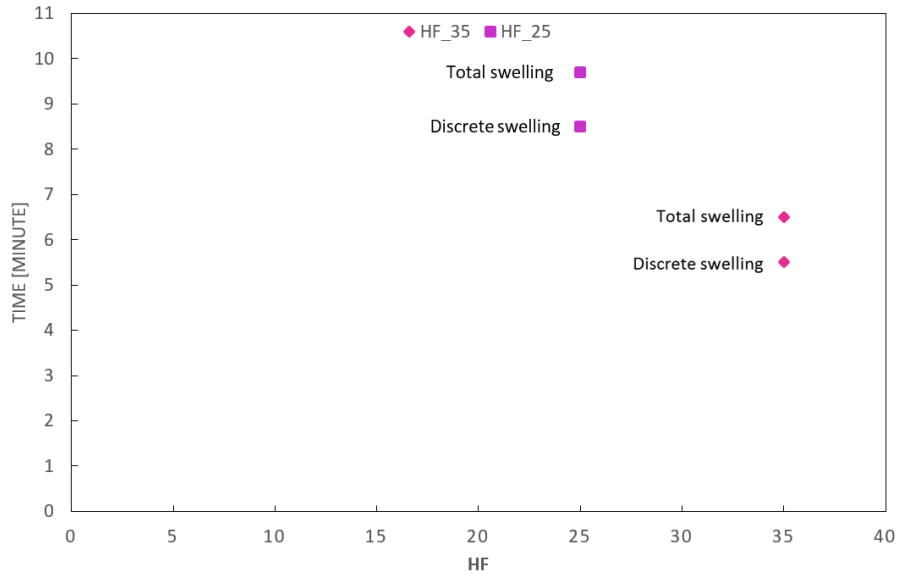


*Figure 5. 4: Discrete activation and total activation time's difference for samples under incident heat flux of 25 and 35 Kw/m2.*

Figures below shows the transition faces of thin intumescent coating from virgin material to the onset of total swelling activation. It can be seen from the photos that discrete activation spots remain at the surface of the coating even after the total swelling activation starts to take place.

*Figure 5. 5: Images of the intumescence process until total swelling activation of thin intumescent coating.*

## 5.2 Swelling rate

It has been noticed that HF_35 tests have higher swelling compared to HF_40 and HF_50 and the influence on that could be seen on the back-steel temperatures of the back steel is much higher for HF_40 and HF_50 than HF_35. This could be explained from the figure below, where it can be seen that to the right-hand side of the dashed lines, the swelling of the HF_50_2 start to stop increasing and even decreased at one point and the influence of that could be seen at the back steel temperature for HF_50_2 tests where it counties to increase rapidly. While for test HF_35_2, swelling curve seems to continue increasing with time until almost the end of the test, and the influence of this can be seen over the temperature of the HF_30_2 as it keeps increasing with any rapid change or in other words increasing steadily.

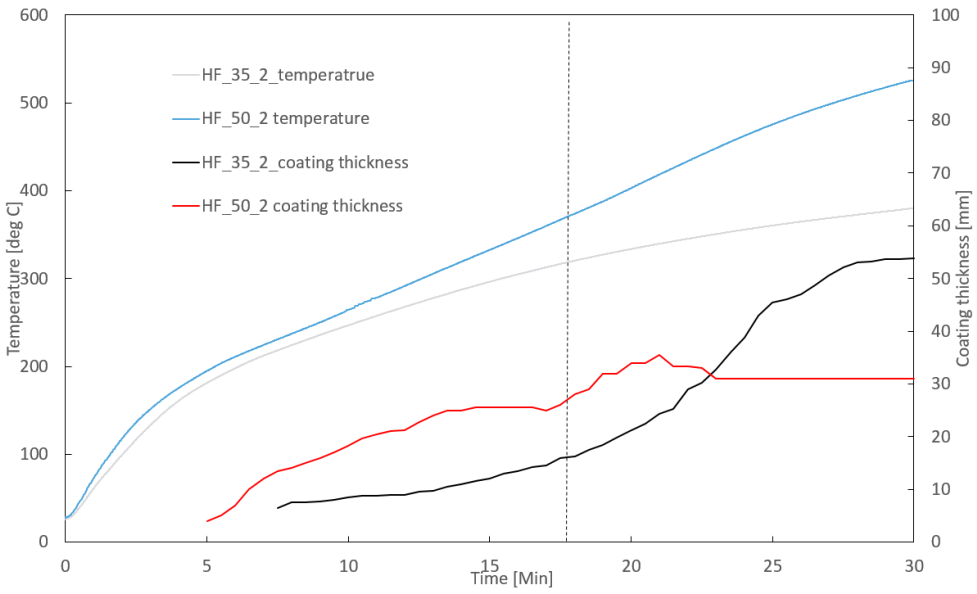


*Figure 5. 6: Comparison between back steel temperatures and swelling curves.*

When comparing the expansion ratios listed in table 4.2, it can be seen that best expansion among the other tests are HF_35 tests, the expansion factors are higher than the rest, Figure 5.8 shows comparison between all the expansion ratios, again it should be highlighted that HF_23, HF_20 and HF_16 tests didn't really swell but expansion factors has been calculated based on the final thickness of the coating after 30 minutes testing.

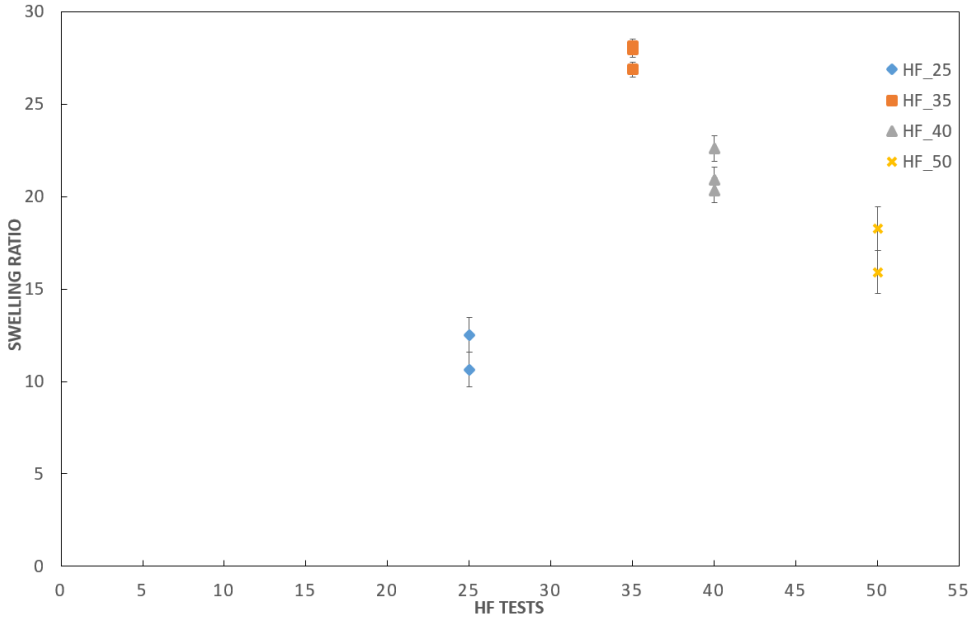


*Figure 5. 7: Expansion ratios for the different tests.*

From Figure 4.6 it can be seen that higher heat fluxes doesn't necessarily lead to higher swellings, HF_35_2 has shown to be the highest expansion among the other tests, it can be seen that it increases steadily until the end of the duration of the tests. While HF_40_2 and HF_50_2 expansion curves don't increase steadily as HF_35 does during the tests. Which can be interpreted as the swelling activation is a heat flux dependent not only a temperature dependent.

Figure 5.8 shows the analysis of readings from 9 different spots for measuring of the final thickness of the swelling. As it can be seen, higher heat fluxes result in higher variation of readings as the coating final thickness is higher and has more variations along the surface of the coating, also it can be seen that HF_35 tests have the higher standard deviation among others, which can be interpreted that the coating final thickness measurements varies the highest compared to other tests as HF_35 tests have the highest coating final thickness. Average values have been taken for the repeated tests for the below Figure.

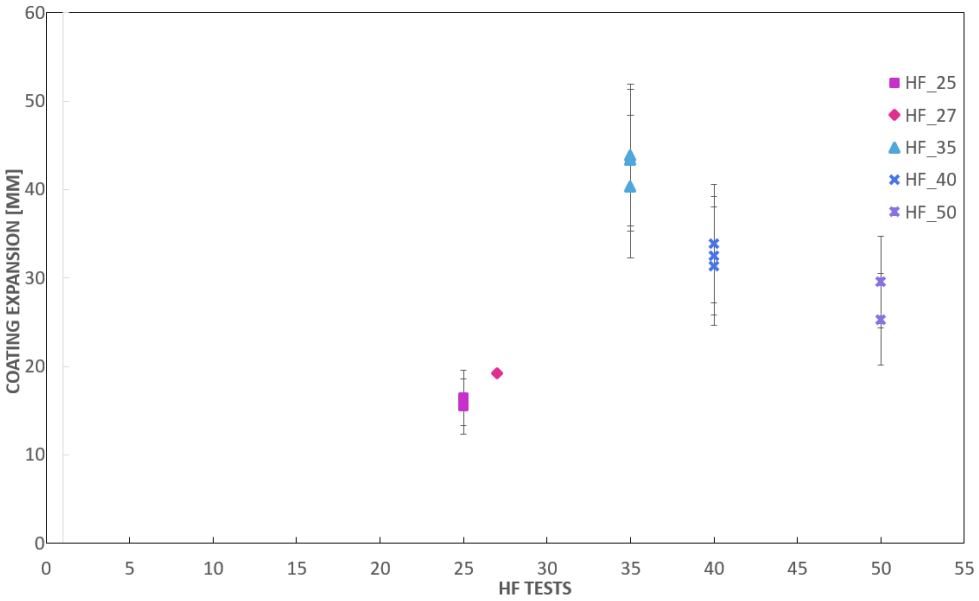


*Figure 5. 8: Coating final swelling thickness measurements variation analysis.*

One of the visual observations that could have affected the swelling of HF_50 and HF_40 is the presence of flames over the surface of the coating, it was noticed that when a high hear flux exposed to the coating a flame appears over the surface. The presence of the flame didn't appear all the time when repeated tests has been done, for example in HF_40_1 test flame appeared over the surface of the coating while for HF_40_2 and HF_40_3 didn't. The same for HF_35 tests, HF_35_1 and HF_35_3 didn't have flame over the surface of the coating but HF_35_2 did have. The presence of the flame is not really clear, and it was beyond the scope of this work, so not that much attention has been given to study the reasons behind this phenomena. However, it's believed that the presence of the flame affected the swelling rate for the mentioned tests. Figures below show the presence of the flame over the surface of the coating.

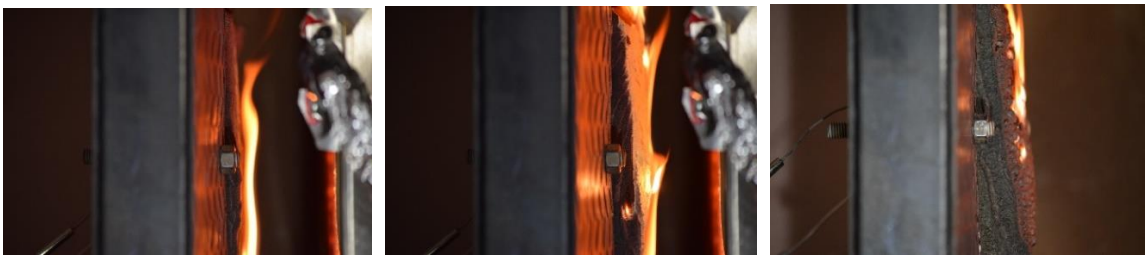

*Figure 5. 9: Flame appearing over the surface of the coating from different tests.*

## 5.3 Unprotected steel

Figure 5.10 below shows the comparison between back steel temperatures for protected, unprotected and heat transfer model back steel temperature. It can be seen that there is very good matching between the heat transfer model and unprotected back steel temperatures, which give a good validation for the model. It can be seen from the Figure below that the back steel temperature significantly reduced by the effect of the coating expansion during the 30 minutes duration of the tests. Back steel temperature difference for unprotected and protected is almost 250 degree Celsius which shows the importance of the intumescent coating in reducing the steel temperatures during a fire. The location of the dash line is located at the onset time obtained from table 4.1 and it can be seen that from that time on the difference between of the back steel temperature between the protected and unprotected steel plate is varying significantly with time which is influenced by the swelling of the coating. The back steel temperature difference of both protected and unprotected steel plates prior to the swelling activation is because of the presence of the coating layer as well as the local activation effect.

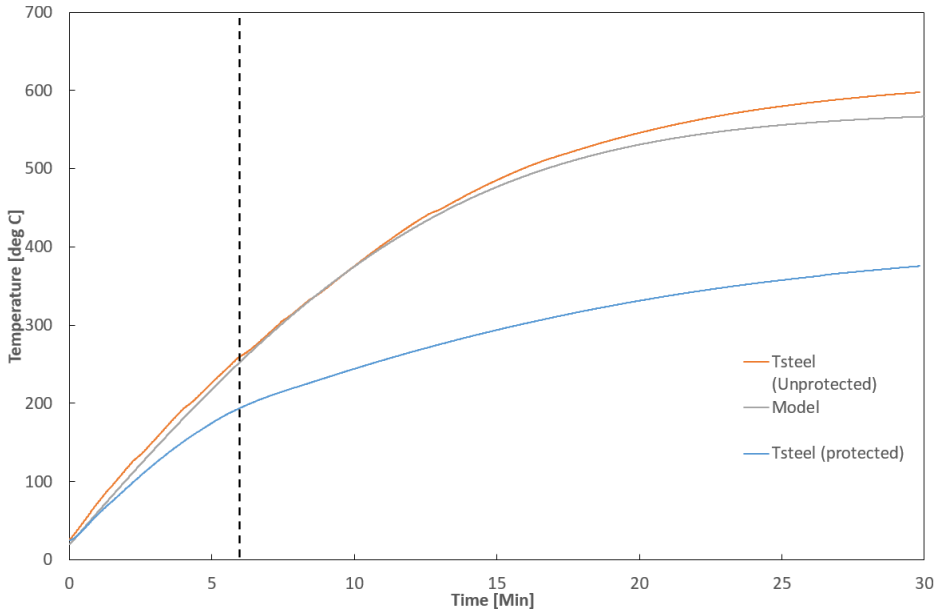


*Figure 5. 10 :HF_35 protected, unprotected and model back steel temperatures.*

Same applies for HF_50 where it can be seen that the predicted temperature and the unprotected steel temperatures shows good matching. Also, it can be seen that there is a significant difference between the back steel temperatures of the protected and unprotected steel plates, there is almost 300 degree Celsius difference which shows again the effectiveness of the intumescent coating.

In addition, it can be seen that the effectiveness of the intumescent coating in reducing the back steel temperatures increased slightly for HF_50 than HF_35, where the final back steel temperature difference between the both tests shows that HF_50 temperature reduction by the intumescent coating is higher than the one for HF_35.

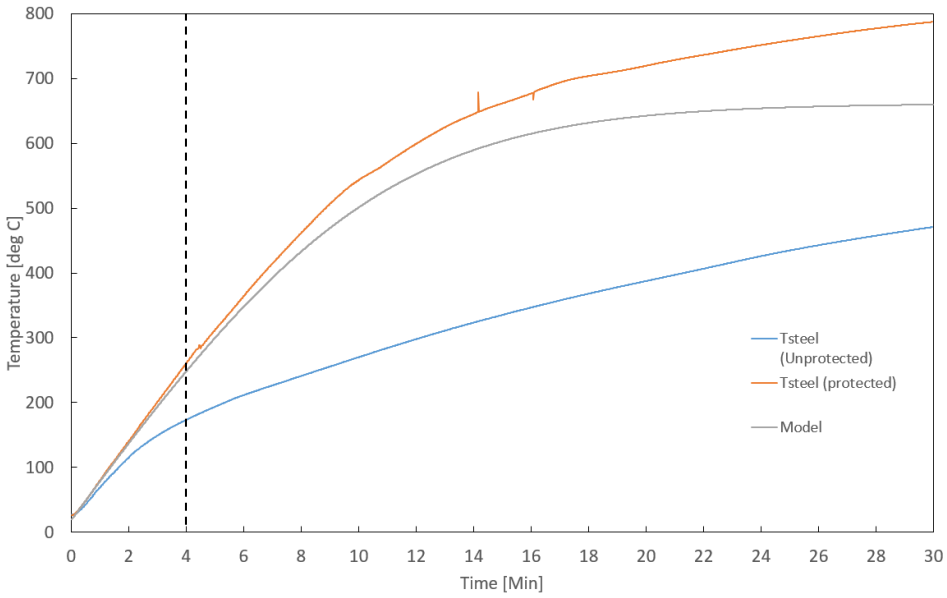


*Figure 5. 11: HF_50 protected, unprotected and back steel temperatures.*

## 5.4 Exploratory work tests with stepwise heating increase

The Figure below shows that the first 15 minutes of the test no activation occurred at all until the heat flux increased up to 50KW/$m^2$, it was stated earlier that the heat flux didn't increase rapidly to 50 kw/$m^2$ but rather than gradually increasing. It can be seen that the temperature curve increased at faster rate to the right hand of the dashed lines compared to the left-hand side. The expansion curve seems to be decreasing slightly at the end, and that could be explained by the fact near to the end of the test the coating stopped swelling and start to "shrink" somehow under the exposure to the heat. It can be seen as well that near 15 minutes of the test, a rapid swelling of the intumescent coating occur and that could be explained due to the large produce of bubbles from the intumescent coating, by minute 20 the rapid increase decrease a bit until minute 25 where a rapid increase of the expansion occur until the expansion stops basically and starts to decrease.

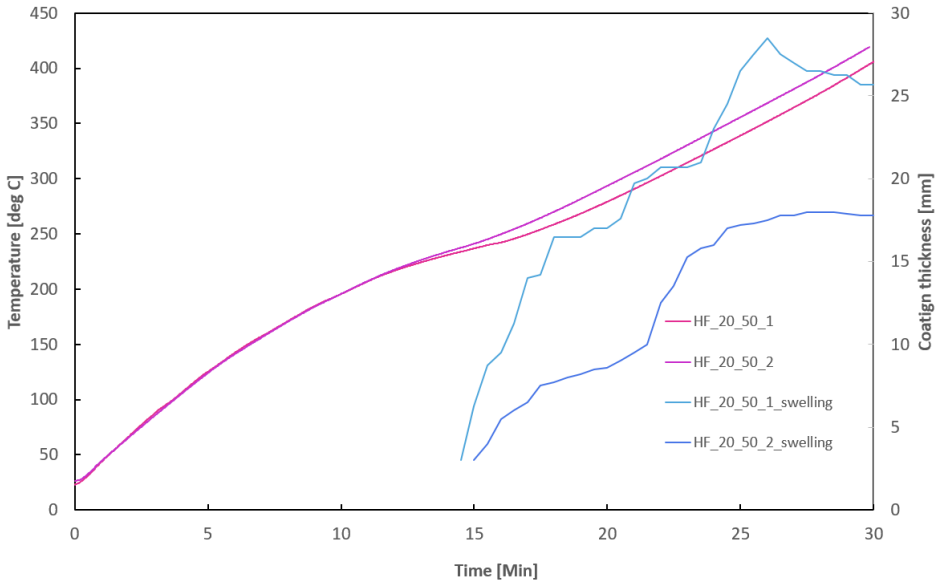


*Figure 5. 12: Temperature and coating expansion comparison.*

## 5.5 Source of uncertainties in data measurement and data analysis

Throughout this work, different uncertainties have been emerged in both data measurements and data analysis. Different uncertainties have emerged due to the following major points:

***Buckling of the sample frame holder*** – One of the difficulties that was faced during this work was the buckling of the steel sample frame holder, where the steel had shown to have buckling and deformation after being exposed to high heat fluxes which would have affected the imposed heat fluxes as the frame would change its relative position from the panel due to the buckling.

***Photo analysis to measure the expansion*** – The swelling curves showed earlier in this work has been analysed manually using different software packages that would analyse the increase of the coating thickness every 30 seconds, this manually analysing technique has added certainties to the readings and the data analysis which could affect the discussion and conclusions. However, a margin of ±2 mm has been considered as uncertainty for the readings from the photo analysis.

***Accumulative thermal energy flux calculation*** – The accumulative energy calculation from the heat transfer model for unprotected steel was compared to the temperature and the swelling curve of protected steel which leave a big uncertainty here about the validity of the model to be used for this work. However, as stated earlier both the intumescent coating and the steel are considered and to be thermally thin and that has been verified in the methodology section.in addition to that, a comparison has been done between back steel temperature for the pre-activation stage with the unprotected steel temperature and both has shown very good matching until the activation occur.

***Sample fabrication*** – The application of the DFT has been done manually as explained in the methodology part and that resulted in variation of the DFT within the same plate, analysis has been and shown in appendix A where a specific criterion has been followed to categorize the plates according to their average thicknesses.

# 6. Conclusion & Future Work

## 6.1 Conclusions

Three different set of tests have been done to study the effectiveness of the activation of the thin intumescent coating studied in this work; study on protected steel samples using set of different heat fluxes, tests on unprotected steel samples using two set of heat fluxes, and exploratory tests imposing stepwise heating increase. The back-steel temperature and the coating swelling of the coating was measured. Heat transfer was established to account for the accumulative thermal energy flux obtained from the area under the curve of the net heat flux imposed on tested samples and showed very good matching with the results of the tests on the unprotected steel samples.

Three important terminologies have been defined based on the results of time to total activation, back steel temperatures, and accumulative energy under the net heat curve which were called the activation temperature, onset time and accumulative thermal energy flux respectively.

***Swelling Activation*** – It has been noticed that based on the heating condition some tested samples show discrete activation spots and some samples don't but rather total swelling occur directly. It was noticed that time to discrete swelling spots increases as the heating condition decrease. It was found out that the back-steel temperatures fall in the range of 180-240 $^{o}$C at the moment of total activation, beside that it has been noticed that intumescent coating under high heat fluxes requires but not necessarily lower activation temperatures and less onset time. Which lead to a point that the swelling activation is heat flux dependent not only temperature dependent.

Besides that, it was shown that the thermal energy flux directly proportionally to the value of the heat flux imposed where it was noticed that intumescent coating requires less accumulative thermal energy flux under high heat fluxes. The range for the accumulative thermal energy flux at the time of the total activation was found to be between 12100 and 13200 [KJ/m$^2$].

The critical heat flux to have total swelling activation is between 23 and 25 KW/m$^2$, this range is in essence the threshold for swelling activation. It was found out that the intumescent coating under heat flux of 35 Kw/m$^2$ has the highest swelling among other tests, it has the highest expansion ratio and the highest final thickness. It was noticed that higher heat fluxes don't necessarily lead to higher expansion ratios. Test exposed to incident heat fluxes above 35 Kw/m$^2$ showed lower swelling rations to those at lower heat fluxes. Also, it was found out at heat fluxes (e.g. 50 Kw/m$^2$) the coating doesn't appear to be effective as 35 Kw/m$^2$ where the back-steel temperatures increase rapidly at the moment the swelling of the coating descends.

***Stepwise heating increase*** – It was found out from the tests under stepwise heating increase that thin intumescent coating tend to activate when a rapid heating condition imposed where rapid bubbling generation occur within the coating which lead to instant expansion of the intumescent coating. Repeated tests showed very good matching in terms of steel temperatures, expansion curves and final expansions.

## 6.2 Future work

Following outcomes of this work, the following could be studied:

- Influence of the DFT on the effectiveness of the swelling activation;
- Influence of different coating type on the effectiveness of the swelling activation;
- Investigation of multiple stepwise heating conditions on the effectiveness of the swelling activation;
- Influence of different heating conditions on bubble generation and bubbling sized could be studied at the moment of the total swelling activation. In addition, the effective thermal conductivity for the thin intumescent coating at the moment of the total activation should be calculated for under the use of the novel test method described here.
- Heat transfer model should be enhanced to account for the intumescent coating to have more reliability of the accumulative thermal energy flux, also the heat losses from the system should be measured using different techniques to have a validation for the for the proposed model.

# References


1. Anderson, C.E. et al., 1985. Intumescent Reaction Mechanisms. *Journal Of Fire Sciences*, 3, pp.161–194. Available At: Http://Jfs.Sagepub.Com/Content/3/3/161.Short.

2. Anon 2014, Hotdisk Thermal Conductivity Analysers. Available At: Http://Www.Thermal-Instruments.Co.Uk/Hotdisk.Htm [Accessed April 2, 2017].

3. Anon 2017, » Using Gypsum Board For Walls And Ceilings Section I. Available at: Https://Www.Gypsum.Org/Technical/Using-Gypsum-Board-For-Walls-And-Ceilings/Using-Gypsum-Board-For-Walls-And-Ceilings-Section-I/ [Accessed March 22, 2017].

4. Anon, ATAD Steel Structure Corporation. Avaliable at: Http:// http://atad.vn/news/fire-protecting-structural-steelwork.

5. Anon, Windsor Tower (Madrid) - Wikipedia. Available at: Https://En.Wikipedia.Org/Wiki/Windsor_Tower_(Madrid) [Accessed March 19, 2017b].

6. Archtoolbox, Spray Applied Fireproofing - Archtoolbox.Com. Available at: Https://Www.Archtoolbox.Com/Materials-Systems/Thermal-Moisture-Protection/Spray-Applied-Fireproofing.Html [Accessed March 22, 2017].

7. Bergman, T.L. Et Al., 2011. *Fundamentals Of Heat And Mass Transfer,* John Wiley & Sons.

8. Bourbigot, S., Le Bras, M., Duquesne, S., And Rochery, M., (2004) "Recent Advances For Intumescent Polymers", Macromol. Mater. Eng., 289, 499

9. Bourbigoti, S., Le Bras, M, Dabrowski, F., Gilman, J. W., And Kashiwagi, T, (2000) "Pa-6 Clay Nanocomposite Hybrid As Char Forming Agent In Intumescent Formulations" Fire Mater. 24, 201.

10. Buchanan A.H., 2001. Structural Design for Fire Safety, John Wiley & Sons.

11. C. Maluk, Et Al., A 2016 .Heat-Transfer Rate Inducing System(H-TRIS)Test Method, Fire Safety Journal.

12. Camino, G., L. Costa & L. Trossarelli, 1985. Study of The Mechanism of Intumescence In Fire Retardant Polymers: Part Vi--Mechanism Of Ester Formation In Ammonia Pol Yphosphate-Pentaerythritol Mixtures" Poly. Deg. And Sta.,12, 213.

13. Camino, G., L. Costa, And G. Martinasso ,1989. Intumescent Fire-Retardant Systems, Poly. Deg. And Stab., 23, 359.

14. CAMINO, G., L. COSTA. 1988. PERFORMANCE AND MECHANISMS OF FIRE RETARDANTS in Polymerswa Review, Poly. Oeg. And Stab., 20, 271.

15. Cirpici, B.K., 2015. Simulating The Expansion Process Of Intumescent Coating Fire Protection, PhD Thesis, Manchester University.

16. Di Blasi, C. & Branca, C., 2001. Mathematical Model For The Nonsteady Decomposition Of Intumescent Coatings. *Aiche Journal*, 47(10), Pp.2359–2370.

17. Elliott, A. et al., 2014. Novel Testing To Study The Performance Of Intumescent Coatings Under Non-Standard Heating Regimes. In *Fire Safety Science*.

18. "Eurocode 1: Actions on struc- tures - Part 1-1. 2002,: General actions - Densities, self-weight, imposed loads for build- ings", EN 1991-1-1.

19. "Eurocode 3: Design of steel structures-Part 1-2. 2005,: General rules- Strcutural; fire design", EN 1993-1-2.

20. Goode, M.G., 2004. Fire Protection Of Structural Steel In High-Rise Buildings. Nist, P.88. Available At: Http://Fire.Nist.Gov/Bfrlpubs/Build04/Art047.Html.

21. Gross,. J et al., 2005. Fire Resistance Tests of Floor Truss Systems, NIST.

22. Horrocks, A. R.,1996. Development In Flame Retardants For Heat And Fire Resistant Textiles The Role Of Char Formation And Intumescence. Poly. Degrad. And Stab., 54, 143.
23. Industrial, C.C.&, 2006. Fire Resistance Of Steel-Framed Buildings. , Pp.3–39.

24. Jimenez, M., Duquesne, S. & Bourbigot, S., 2006. Intumescent Fire Protective Coating: Toward A Better Understanding Of Their Mechanism Of Action. *Thermochimica Acta*, 449(1–2), Pp.16–26.

25. LE BRAS, M., BUGAJNY,M., LEFEBVRE, J., AND BOURBIGOT, S., 2000. Use Of Polyurethanes As Char-Forming Agents In Polypropylene Intrumescent Formulations, *Polymers International*, 49,1115.

26. Luchreni, A. et al., 2016. Experimental Study Of The Behaviour Of Steel Structures Protecetd By Different Intumescent Coatings And Exposed To Various Fire Scenarios, Proceedings Of The 9th International Conference On Structures In Fire Pp. 1065-1072.

27. Mariappan, T., 2015. Recent Developments Of Intumescent Fire Protection Coatings For Structural Steel: A Review.

28. Mcnamee, R.J. et al., 2016, The Funtion Of Of Intumescnt Paint For Steel During Different Fire Exposure. SP Report.

29. Mesquita, L.M.R., Piloto, P.A.G. & Vaz, M.A.P., 2007. An Experimental Study Of Intumescent Fire Protection Coatings. *European Coatings: Fire Retardant Coatings II, Berlin, Germany*.

30. Mroz, K., Hager, I. & Korniejenko, K., 2016. Material Solutions For Passive Fire Protection Of Buildings And Structures And Their Performances Testing. *Procedia Engineering*, 151, Pp.284–291. Available At: Http://Dx.Doi.Org/10.1016/J.Proeng.2016.07.388.

31. Norgaard K P., 2014. Investigation of an Intumescent Coating System in Pilot and Laboratory-Scale Furnaces Ph.D. Thesis, Technical University of Denmark.
32. Purkiss, J.A. & Li, L.-Y., 2013. *Fire Safety Engineering Design Of Structures, Third Edition*.

33. Richardson, K., 2003. Historical Evolution of Fire Protection Engineering, *History of Fire Protection Engineering*, National Fire Protection Association, Quincy, MA.

34. SFPE. 2000. SFPE Engineering Guide to Performance Based Fire Protection Analysis and Design of Building.

35. Skowronski, W., 2001. Fire Safety of Metal Structures.

36. Steelconstruction.Info, 2016. Fire Protecting Structural Steelwork. Available At: Http://Www.Steelconstruction.Info/Fire_Protecting_Structural_Steelwork#Concrete_Encasement [Accessed March 23, 2017].

37. VANDERSALL H. L. 1971 Intumescent Coating Systems, Their Development and Chemistry, J. FIRE & FLAMMABILITY, VOL. 2, PP. 97-140.

38. Wang Y.C., 2005. Goransson U., Holmstedt, G And Omrane A., A Model For Prediction Of Temperatures In Steel Structures Protected By Intumescent Coating, Based On Tests In The Cone Calorimeter, Proceedings Of The 8th International Symposium On Fire Safety Science, Beijing, China, Pp. 235-246.

39. Wang, H., 1995. Heat Transfer Analysis Of Components Of Construction Exposed To Fire. Available At: Http://Usir.Salford.Ac.Uk/14780/.

40. Wang, L. et al., 2015. Exprirmental Study Of Heat Transfer In Intumesacent Coatings Exposed To Non-Standard-Furnace Curve. Fire Technology, 51, 627-643.

41. Wang, Y., 2002. Steel And Composite Structures: Behaviour And Design For Fire Safety.

# APPENDIX A
# DFTs THICKNESSES measurements

*Table A 1: DFTs measurement analysis.*

| Sample Label | DFTs measurements | | | | | DFT mean | DFT std dev | DFT max | DFT min |
|---|---|---|---|---|---|---|---|---|---|
| | **#1** | **#2** | **#3** | **#4** | **#5** | | | | |
| | **[µm]** | **[µm]** | **[µm]** | **[µm]** | **[µm]** | **[µm]** | **[-]** | **[µm]** | **[µm]** |
| **HF_50_1** | 1460 | 1680 | 1570 | 1510 | 1610 | 1566 | 85.62 | 1680 | 1460 |
| **HF_50_2** | 1710 | 1390 | 1700 | 1610 | 1680 | 1618 | 133.30 | 1710 | 1390 |
| **HF_40_1** | 1520 | - | 1400 | - | 1400 | 1440 | 69.28 | 1520 | 1400 |
| **HF_40_2** | 1320 | 1710 | 1380 | 1710 | 1570 | 1538 | 182.13 | 1710 | 1320 |
| **HF_40_3** | 1640 | 1730 | 1280 | 1670 | 1790 | 1622 | 199.67 | 1790 | 1280 |
| **HF_35_1** | 1500 | - | 1600 | - | 1400 | 1500 | 100 | 1600 | 1400 |
| **HF_35_2** | 1500 | 1330 | 1490 | 1690 | 1720 | 1546 | 160.41 | 1720 | 1330 |
| **HF_35_3** | 1560 | 1690 | 1720 | 1360 | 1450 | 1556 | 153.72 | 1720 | 1360 |
| **HF_27** | 1640 | 1380 | 1240 | 1540 | 1640 | 1488 | 174.7 | 1640 | 1240 |
| **HF_25_1** | 1410 | 1280 | 1200 | 1370 | 1270 | 1306 | 83.85 | 1410 | 1200 |
| **HF_25_2** | 1290 | 1640 | 1250 | 1530 | 1540 | 1450 | 170.44 | 1640 | 1250 |
| **HF_23_1** | 1550 | 1040 | 1560 | 1330 | 1660 | 1428 | 248.13 | 1660 | 1040 |
| **HF_23_2** | 1090 | 1440 | 1190 | 1420 | 1550 | 1338 | 190.71 | 1550 | 1090 |
| **HF_20** | 1240 | 1340 | 1590 | 1530 | 1660 | 1472 | 175.98 | 1660 | 1240 |
| **HF_16** | 1520 | - | 1400 | - | 1400 | 1440 | 69.28 | 1520 | 1400 |
| **HF_20_50_1** | 1700 | 1490 | 1700 | 1500 | 1560 | 1590 | 103.92 | 1700 | 1490 |
| **HF_20_50_2** | 1270 | 1600 | 1290 | 1700 | 2000 | 1572 | 304.58 | 2000 | 1270 |